A Critical Review of Thermal Management Models and Solutions of Lithium-ion Batteries for the Development of Pure Electric Vehicles

Qian Wang, Bin Jiang, Bo Li, Yuying Yan*

Fluids & Thermal Engineering Research Group, Faculty of Engineering,

University of Nottingham, UK

Corresponding author: yuying.yan@nottingham.ac.uk

Abstract

Power train electrification is promoted as a potential alternative to reduce carbon intensity of transportation. Lithium-ion batteries are found to be suitable for hybrid electric vehicles (HEVs) and pure electric vehicles (EVs), and temperature control on lithium batteries is vital for long-term performance and durability. Unfortunately, battery thermal management (BTM) has not been paid close attention partly due to poor understanding of battery thermal behaviour. Cell performance change dramatically with temperature, but it improves with temperature if a suitable operating temperature window is sustained. This paper provides a review on two aspects that are battery thermal model development and thermal management strategies. Thermal effects of lithium-ion batteries in terms of thermal runaway and response under cold temperatures will be studied, and heat generation methods are discussed with aim of performing accurate battery thermal analysis. In addition, current BTM strategies utilised by automotive suppliers will be reviewed to identify the imposing challenges and critical gaps between research and practice. Optimising existing BTMs and exploring new technologies to mitigate battery thermal impacts are required, and efforts in prioritising BTM should be made to improve the temperature uniformity across the battery pack, prolong battery lifespan, and enhance the safety of large packs.

Keywords: Low carbon vehicles, Lithium-ion battery thermal management, heat pipe, pure electric and hybrid cars

1. Introduction

Transportation has become the most growing factor of the world's fuel consumption taking up 49% of oil resources [1]. The efficiency of oil utilisation in vehicles is fairly low, so energy saving strategies in transportation will help reduce unnecessary energy consumption without providing extra utility and services [2]. One of the most distinctive energy saving ideas is the promotion of clean or green energy vehicles. Great attention has been paid to hybrid electric vehicles (HEV), plug-in hybrid electric vehicles (PHEV), and pure electric vehicles (EVs) as potential alternatives to reduce carbon intensity of transportation. It is claimed that these vehicles provide solutions in zero-carbon emissions [3], offer the best possibilities for the use of new energy sources, and benefit long-term energy savings [4-6]. Andersen et al. [7] pointed out that EV reduces up to 20% in GHG emissions and further up to 40% if the electricity is generated by renewable energies. Endo [8] predicted that high efficiency vehicle developments may cut CO_2 emissions to 2/3 of the level in 1990 by 2050. More importantly,

opportunities are offered to EVs, since the US government offers 2.5 billion funding and grants for a variety of EV related companies, and China shifts the focus to develop EV related economic and energy policies [9].

The fundamental challenge for clean energy vehicles to be commercialised is energy storage. Developing a proper battery pack for the vehicle to achieve high power and high energy is essential. Rechargeable lithium-ion batteries are well suited for HEVs and EVs, but they have not yet been widely adopted in automotive industry due to barriers such as cost, safety, and low temperature performance coupled to thermal effects [10]. Battery thermal management (BTM), which is a critical issue for the development of pure electric vehicles, typically pure electric passenger cars [200-2002], has received little attention during the last few years because the understanding of lithium-ion battery thermal issues is lacking. This paper will focus on two aspects of lithium-ion batteries applied to HEVs and/or EVs, namely, the development of battery models and the existing thermal management strategies. Thermal issues such as safety, thermal runaway, and sub-zero temperature operating performance are investigated and discussed. The approaches of battery models in terms of thermal-electrochemical or thermal-electrical coupled and decoupled models will be reviewed and the heat generation is in particular emphasised in order to determine the accuracy of battery thermal analysis. The existing BTM strategies are then investigated so that the imposing challenges and critical gaps between commercial manufacturers and developers can be identified. Eliminating battery thermal impacts by optimising existing BTMs and exploring new technologies is encouraged, and prioritising BTM for HEVs and EVs seems critical in minimising the temperature variations across the batter pack, prolonging battery life cycle, and improving the safety of large packs.

2. Lithium-ion Batteries for Hybrid/Pure Electric Vehicles

2.1. General Considerations

EV, which was invented ahead of the first gasoline-powered vehicle, consists of mainly four elements: an energy source (the battery), a power convertor, an electric motor, and a mechanical transmission [11]. A vehicle driven by an electric motor is much more efficient than an engine-driven vehicle, for that the motor has high efficiency over 90% compared to 30% obtained by the engine [12]. Other merits such as a high-torque at low revolution speed, quicker torque response, and recovering kinetic energy into electricity from braking torque are also favourable. Shimada [13] compared the energy efficiency of FCV (fuel cell vehicles), HEV (hybrid electric vehicles), CNG (compressed natural gas), and BEV (battery electric vehicle) based on the input energy per 1km during 10-15 mode driving cycle test [14]. BEV (or EV) has shown to have the lowest input energy proportional to CO_2 discharge and the highest fuel economy. The heat loss of EV, in addition, is significantly small compared to that from the engine vehicle. However, the fuel density of batteries in comparison with liquid fuel or gas fuel retains extremely low, which implies that EV has to carry a large amount of battery cells in order to achieve the same performance offered by the engine-vehicle.

A Ragone plot for various batteries, electrochemical capacitors, and fuel cells (including recently reported solid oxide fuel cell (SOFC) [15]) made for many applications ranging from consumer electronics to vehicles is provided in Fig. 1. The specific power translates to the acceleration in a vehicle; while the specific energy, the driving range. It can be noted that lithium-ion batteries are superior to other cell chemistries for EV, PHEV (plug-in hybrid electric vehicle) and HEV but no battery system can compete with gasoline (i.e. internal combustion or IC-Engine). As reported by Linden [16], lithium-ion batteries are well-suited for vehicle applications because they have nearly

twice the amount of specific energy and energy density (150 Wh/kg and 400 Wh/L respectively) relative to the practical nickel-metal hydride (NiMH) batteries (75 Wh/kg and 240 Wh/L), which have dominated the HEV market.

Apart from acceleration and driving performance, other criteria such as cost, range, and lifespan, as well as safety, are also critical. The cost of an EV battery is significant, arguably and prohibitive. $/kWh is an important quantity in evaluating cost. The United States Advanced Battery Consortium (USABC) outlined $/kWh goals for battery technology to reach a commercially viable level, which is $200-300/kWh versus current costs of $750-1000/kWh [17]. Cluzel and Douglas [18] presented both conservative and optimistic scenario results of battery pack cost based on different EV classes and the reported cost ranges from $587-1,327/kWh in 2011. Additionally, Gaines and Cuenca [19] broke down the materials cost of a 10Ah lithium-ion high power cell and pointed out that cathode, separator and electrolyte contribute the most to the total battery cost, taking up 28%, 23% and 20% respectively. It is stated in [20-22] that lithium-ion batteries have not yet achieved the potential of cost reductions and the search for reducing potential cost is encouraged by material substitution, increased packaging efficiencies, process development, increased manufacturing yields or inexpensive production.

Table 1 lists the types of storage batteries currently used or to be used in EVs. Notably, high-temperature batteries, which have been developed for quite a few years and now in pilot production, have not been used in EV productions. Therefore, only ambient operating temperature batteries are considered for EVs to ensure good performance and safety. A suitable lifespan for a practical battery is suggested to be 1000 cycles or about 3-4 years. Open-circuit voltage is also crucial which determines the required number of cells to form a battery pack reflecting battery complexity and potential reliability. The higher the voltage becomes, the better the ratio of the active components in the cell over the passive containing materials. From Table 1, lithium-ion batteries seem to be the best among other cell chemistries due to high energy and power density, long life cycles, ambient operating temperature, and high open-circuit cell voltage. Lithium-ion batteries can store more energy per mass compared to NiMH, and achieves high cell voltage of 3.6V in contrast with 1.23V obtained by NiMH. More importantly, lithium-ion refers to the family of battery chemistry, as shown in Table 2, which indicates material flexibility and potential in cost reduction through material substitution.

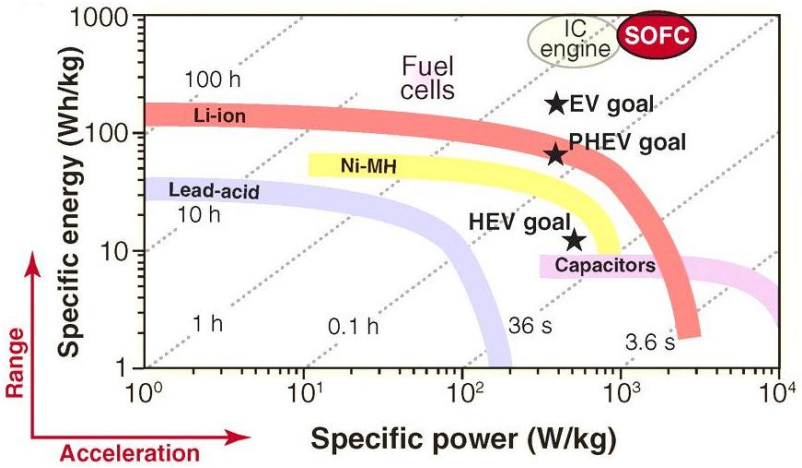

Figure 1: Ragone plot of various electrochemical energy storage and conversion devices [23] including recently reported SOFC [15].

Table 1: Properties of electric vehicle batteries that operate at ambient temperature ([24]).

	Q_{max} (Wh/kg)	P_{max} (W/kg)	t (min)	N	$/kWh	V (V)
Lead-acid	35	150	/	1000	60	2.1
Advanced lead-acid	45	250	/	1500	200	/
Valve regulated lead-acid	50	150+	15	700+	150	/
Metal foil lead-acid	30	900	15	500+	/	/
Nickel-iron	50	100	/	2000	150-200	1.2
Nickel-zinc	70	150	/	300	150-200	1.7
Nickel-cadmium	50	200	15	2000	300	1.2
Nickel-metal hydride (NiMH)	70	200	35	2000+	250	1.23
Lithium-ion	120-150	120-150	<60	1000+	150	3.6
Aluminium-air	220	30	/	/	/	1.5
Zinc-air	200	80-140	/	200	100	1.65

Note:
Q_{max} – maximum energy density;
P_{max} – maximum power density;
t - fastest 80% recharge time;
N – 80% discharge cycles before replacement;
$ - estimated large-scale production cost per kWh;
V – open-circuit cell voltage.

Table 2. The major components of lithium-ion batteries and their properties [25, 26]

Abbrev.	**LCO**	**LNO**	**NCA**	**NMC**	**LMO**	**LFP**	**LTO**
Name	Lithium cobalt oxide	Lithium nickel oxide	Lithium nickel cobalt aluminium oxide	Lithium nickel, manganese cobalt oxide	Lithium manganese spinel	Lithium iron phosphate	Lithium titanate
Positive electrode	$LiCoO_2$	$LiNiO_2$	$Li(Ni_{0,85}Co_{0,1}Al_{0,05})O_2$	$Li(Ni_{0,33}Mn_{0,33}Co_{0,33})O_2$	$LiMn_2O_4$	$LiFePO_4$	LMO, NCA, …
Negative electrode	Graphite	Graphite	Graphite	Graphite	Graphite	Graphite	$Li_4Ti_5O_{12}$

Cell voltage (V)	3.7-3.9	3.6	3.65	3.8-4.0	4.0	3.3	2.3-2.5
Energy density (Wh/kg)	150mAh/g	150	130	170	120	130	85
Power	+	o	+	o	+	+	++
Safety	-	o	o	o	+	++	++
Lifetime	-	o	+	o	o	+	+++
Cost	--	+	o	o	+	+	o

2.2. Mechanism and Configuration

The mechanism of a lithium-ion battery is given by Fig. 2. Lithium-ions (Li^+) move from the negative electrode (cathode) to the positive electrode (anode) via a separator diaphragm to form a discharge cycle, and vice versa when charging. The cathode is usually made of carbon, and the most commercially popular material is graphite. The anode is a lithium containing compound and is generally one of three materials: a layered oxide (e.g. lithium cobalt oxide – $LiCoO_2$), a polyanion (e.g. lithium iron phosphate – $LiFePO_4$) or a spinel (e.g. lithium manganese oxide – $LiMn_2O_4$). The electrolyte refers to a solution of lithium salt in a non-aqueous solvent such as ethylene carbonate or diethyl carbonate. The current collector for negative and positive electrode is made of copper (Cu) and aluminium (Al) respectively. Taking $LiMn_2O_4$/graphite as an example, the electrochemical reactions occurring at the electrode/electrolyte interfaces are described below.

Composite positive electrode:

$$Li_{y-x}Mn_2O_4 + xLi^+ + xe^- \underset{charge}{\overset{discharge}{\rightleftharpoons}} Li_yMn_2O_4$$

Composite negative electrode:

$$Li_xC_6 \underset{charge}{\overset{discharge}{\rightleftharpoons}} Li_0C_6 + xLi^+ + xe^-$$

As illustrated in Fig. 2, Li^+ is inserted into solid particles of the anode and de-inserts from solid particles of the cathode during discharge. Lithium-ion diffusion in the solid phase and the electrolyte depletion will always limit cell discharge. Significantly, heat is generated within the cell and dissipated to the surroundings in all directions. If the heat is dissipated only through the graphite on the top of the two electrodes, temperature gradient will be developed along the cell height leading to non-uniform electrode reaction rates.

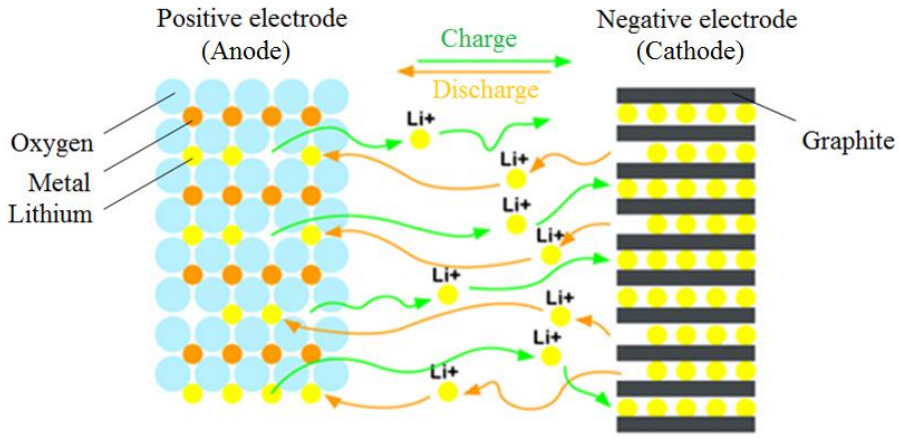

Figure 2: Lithium-ion battery mechanism during charge and discharge.

Three configurations of lithium-ion battery cell are shown in Fig. 3. Both cylindrical and prismatic lithium-ion batteries at cell-, module-, and pack-level for EVs have been demonstrated by Fig. 4. Purely for the purpose of cooling, the prismatic type seems to be most suitable for vehicles because a relatively large surface area in dissipating heat from cell interior to the exterior is available. However, due to factors such as production maturity, availability, safety, lifecycle, and cost, cylindrical cells are still in frequent uses (e.g. Tesla, BMW mini). For automotive applications, cells are connected together in different configurations and packaged with control and safety circuitry to form a battery module. Modules are then combined with additional control circuitry, a battery thermal management system, and power electronics to form a battery pack. Fig. 5 displays a complete lithium-ion battery pack for a PHEV made by A123 Systems [27].

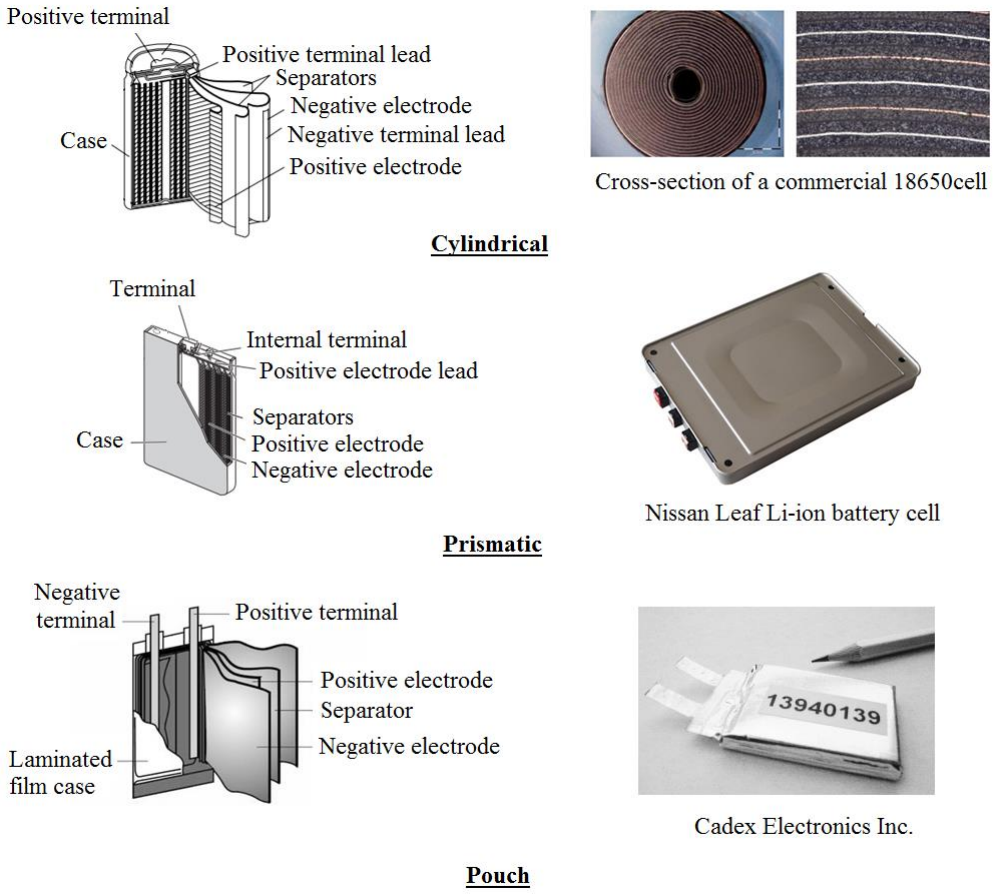

Figure 3: Battery cell configurations.

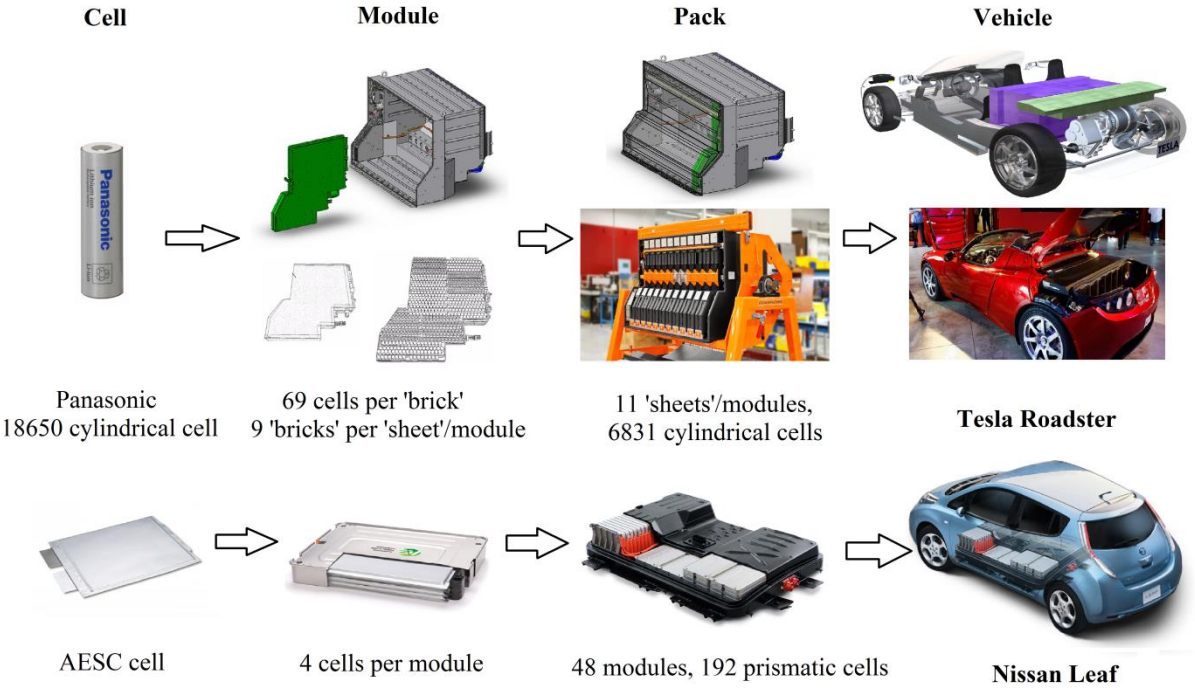

Figure 4: Lithium-ion battery cell-, module-, and pack-level demonstrated by two vehicle examples: Tesla Roadster [28, 29] and Nissan Leaf [30].

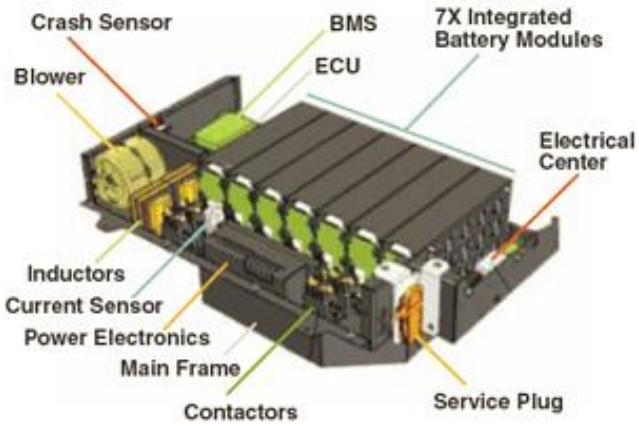

Figure 5: Lithium-ion battery pack for a PHEV (A123 Systems) [27].

2.3. Market Penetration and Potential

The future development of EV can be predicted by introducing major work done by specialist niche manufactures. Table 3 summarises major EV productions currently available/unavailable in the market. It seems that NiCd (Citroën, Ford, Peugeot and Renault) and NiMH (GM, Honda and Toyota) were the most favourite two for EV batteries back in 2000. The inconsistent aim set by the manufacturers indicates the immaturity of battery technology, such that scarce evidence of EV mass production to the public was seen. However, in recent 5 years, lithium-ion batteries become the top candidate in EV manufacturers due to lightweight, higher energy and power density, improved nominal range, and reasonable fast charging time. The cases of commercial success of EVs are listed in Table 3 and these may have suggested that lithium-ion batteries will possibly be a preferred solution for overcoming the challenges of energy storage and driving range encountered by many battery powered vehicles.

Table 3: List of major EV productions currently available and no longer available (by 2014)

Model Type	Battery Type	Battery Weight (kg)	Top speed (km/h)	Nominal Range (km)	Charge Time (h)	Sale/lease Price	Market Release Date
Available in [31-40]							
BMW i3	22 kWh Lithium-ion	230 [41]	150	130-160	0.5-9	$52,000 [42]	2013
BYD e6	75 kWh $LiFePO_4$	500 [43]	140	330	10-20min	$52,000 [44]	2010
Chevrolet Spark EV	21.3 kWh nanophosphate Lithium-ion	254 [45]	144	132	0.33-7	From $12,170 [46]	2013

Citroën C-Zero (*also called* Mitsubishi i-MiEV)	16 kWh Lithium-ion	240 (200 [47])	130	100-160 (170)	0.5-7 (0.5-14)	$48,000 [48] (>$38,000) [49]	2010 (2009)
Ford Focus	23 kWh Lithium-ion	300 [50]	135	122	3-4, 18-20	$35,170 [51]	2011
Nissan Leaf	24 kWh Lithium-ion	294 [52]	150	117-200	0.5-20	$35,430	2010
Tesla Model S	60-85 kWh Lithium-ion	535-556 [53]	193-214	370-426	1.5-20 min	$63,570 [54]	2012
Venturi Fetish	54 kWh Lithium-ion polymer	450 [55]	200	340	3-8	$400,000	2006
Volkswagen e-Up!	18.7 kWh Lithium-ion	230 [56]	130	160	0.5	$34,500	2013

general information from [24, 57]

Ford Th!nkCity	11.5 kWh NiCd	260 [58]	90	85	5-8	/	1999 -2002
GM EV1	16.2 kWh Lead-acid	594 [59]	129	95	6	$399 per month	1996 -2003
GM EV1	26.4 kWh NiMH	481 [60]	129	130	6	$480 per month	1996 -2003
Honda EV Plus	26.2 kWh NiMH	374	129	190	6-8	$455 per month	1997 -1999
Nissan Hypermini	15 kWh Lithium-ion	/	100	115	4	$23,350 -36,000	1999 -2001
Nissan Altra EV	32 kWh Lithium-ion	365 [61]	120	190	5	$50,999	1998 -2000
Peugeot 106 électrique (*also called* Citroën Saxo électrique)	12 kWh NiCd	/	90 (91)	150 (80)	7-8 (7)	$14,700 -27,000 ($12,300 excluding batteries)	1995 -2003
Renault Clio Electric	11.4 kWh NiCd	/	95	80	/	$16,000 -27,400	/
Toyota RAV 4	27 kWh NiMH	380	125	200	10	$45,000	1997 -2002

Tesla Roadster	53 kWh Lithium-ion	450 [62]	209	390	3-5	>$92,000	2008 -2012

Note: charge time varies depending on the charging method. Long hours of charging may be needed with conventional charger (e.g. onboard charger, charged from household); short period of charging can be realised by a quick charger system (50-80% of battery capacity charged) (e.g. AC/DC fast charging station, Tesla Superchargers, etc) or battery swap (1.5min demonstrated by Tesla Motor).

3. Thermal Analysis of Lithium-ion Batteries

3.1. Safety and Thermal Runaway

For high voltage batteries such as lithium-ion battery in particular, prioritising safety at every step of the battery development including material selection, cell design, electronic controls and module assembly is essential but challenging. According to Doughty and Roth [63], safety is required to be evaluated at every level, i.e. the cell, the module, the pack and ultimately the vehicle level. This is because failure at one level will escalate to much more severe failures at a higher level. The international standard ISO 6469 [64] addresses safety specifications for electrically propelled road vehicles including onboard electrical energy storage (Part 1), functional safety means and protection against failures (Part 2), and protection of persons against electrical hazards (Part 3). Safety devices are required to be incorporated into EV batteries to protect against off-normal operations and manage consequences of heat and gas generation. One of these devices is battery management system that regulates electrical distribution and prevents from over-voltage, under-voltage, excessive current, as well as elevated temperature.

Various battery chemistries have different responses to failure, but the most common failure mode of a cell under abusive conditions is the generation of heat and gas [65]. The possible exothermic reactions and thermal stability of lithium-ion batteries have been reviewed in [10] and [63]. Table 4 summarises the identified reaction of the components used in a lithium-ion battery. It shows that the components are completely stable below 80°C, but once the temperature reaches to 120-130°C, the passivation layer (SEI – solid-electrolyte interface) starts dissolving progressively in the electrolyte causing the electrolyte to react with the least protected surface of graphite generating heat.

Table 4: Thermal stability of components used in a lithium-ion battery (values measured with differential scanning calorimetry on electrodes) [26].

Temperature (°C)	Associated reactions	Energy (J/g)	Comment
120-130	Passivation layer	200-350	Passive layer breaks, solubilisation starts below 100°C
130-140	PE separator melts	-90	Endothermic
160-170	PP separator melts	-190	Endothermic
200	Solvents-$LiPF_6$	300	Slow kinetic

200-230	Positive material decomposition	1000	O2 emission reacts with solvents
240-250	LiC_6 + binder	300-500	
240-250	LiC_6 + electrolyte	1000-1500	

Roth et al. [66] tested three different lithium-ion cells (SONY/GEN1/GEN2) under elevated temperature abusive conditions. Data summarised by Doughty [67] illustrates a general path to thermal runaway in lithium-ion cells which can be categorised into three stages (Fig. 6): 1) initial thermal runaway regime; 2) cell venting; 3) cell runaway and explosive decomposition. Thermal runaway describes the condition when elevated temperature triggers heat-generating exothermic reactions and potentially increases the temperature causing more deleterious reactions [10]. If no heat dissipation method is available, the internal cell temperature will continue increasing rapidly. Once the temperature exceeds the onset temperature, the heat release will be accelerated due to increased electrolyte reduction at the anode (Stage 2). Additional heating may cause the cell to generate more than 10°C/min self-heating rate leading to thermal runaway (Stage 3). As a consequence, this progresses into battery fire and explosion. Examples of EV incidents listed in Table 5 may give an idea of how car crash or charging/discharging batteries leads to potential overheating or fire explosion. In order to improve lithium-ion battery safety, shutdown separators or pressure releasing devices, safer electrolytes and positive electrode materials, special additives and coatings [68], and an appropriate thermal management strategy are suggested to provide additional safety by limiting thermal runaway and preventing cell from rapid self-heating.

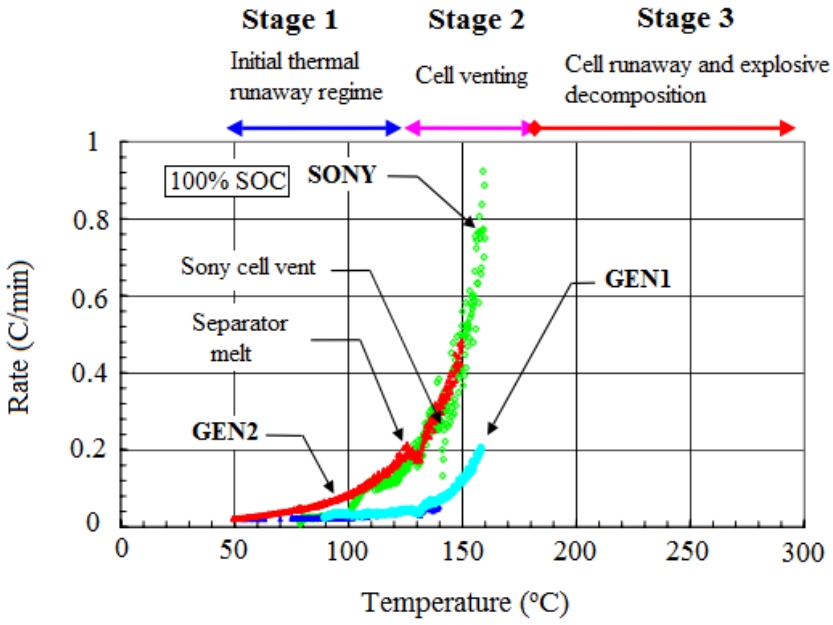

(a)

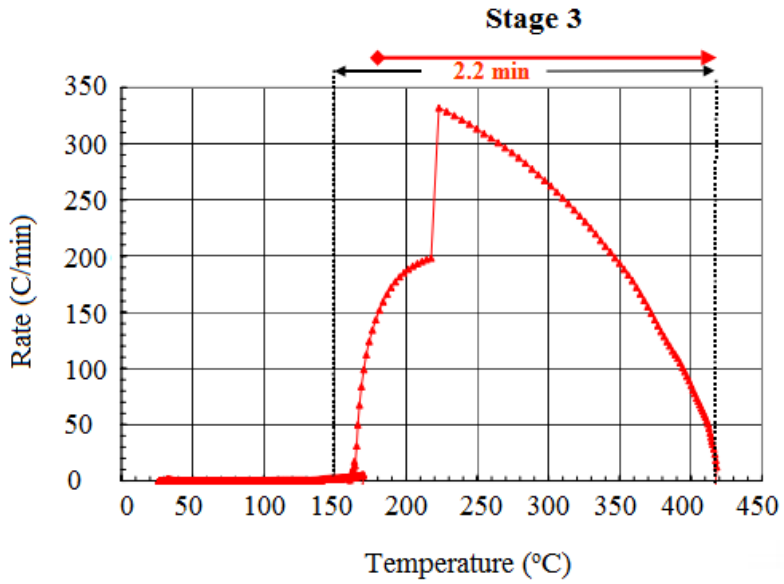

(b)

Figure 6: Illustrating three stages of the thermal response (thermal runaway path) obtained from SONY/GEN1/GEN2 lithium-ion cell [67]: (a) Stage 1-2 in scope; (b) Stage 3.

Table 5: EV incidents

EV Type	**Incident**	**Place & date**	**Investigation summary**
BYD e6	Caught fire after car crash	Shenzhen, China, 2012	Electric arcs caused by short circuit; however 72 out of 96 (75%) single cell batteries did not catch on fire and no flaws in safety design [69]
Chevrolet Volt	Caught fire after crash test	USA, 2011	No higher risk of fire than gasoline-powered vehicles according to National Highway Traffic Safety Administration (NHTSA) [70]
Dodge Ram 1500 PHEV	Overheated battery packs	2012	No injuries, Chrysler recalled as a precaution [71]
Fisker Karma	Home fire in Texas and a fire incident in parking lot in California	Texas and California, 2012	Unknown; Internal fault made the fan to fail, overheat and started fire, not lithium-ion battery pack [72]
Mistubishi i-MiEV	Caught fire at Mizushima battery pack assembly plant when charging/discharging; battery cells in an Outlander PHEV in	2013	Problem related to a change in manufacturing process, the cause has not been officially announced [73]

	Yokohama overheated and melted		
Tesla Model S	Caught fire after hitting debris on highway	Kent, Washington, 2013	Fire began in the battery pack but potential damage was avoided due to isolation of fire barriers inside the battery pack, fire risks are lower when driving a car powered by a battery than that powered by gasoline [74]
Zotye M300 EV	Caught fire	Hangzhou, China, 2011	Lack of quality during manufacturing, problems include leaking of battery cells, insulation damage between battery cells and container, short circuits [75]

3.2. Sub-zero Temperature Performance

Sub-zero climate will make the battery efficiency drop leaving the discharge capacity minimal [76]. This directly affects vehicle mobility and driving range, and subsequently, the life cycle. A good example of this is 2012 Nissan Leaf, which has only 63 miles at -10°C whereas 138 miles under ideal condition [77]. For pure EVs, due to the fact that no combustion engine was present to provide heating, a significant proportion of battery energy will be used for heating the battery and the cabin, shortening the driving range even more by 30–40%. USABC [78] suggests the testing manual for EV batteries, which can be categorised into well-performed battery in cold weather if it absorbs a fast charge from 20% to 60% depth of discharge (DOD) or 40% to 80% state of charge (SOC) in 15min. According to QC/T 743-2006 [79], the discharge capacity requirement for lithium-ion battery at -20°C should be no less than 70% of its rated capacity. However, few batteries are capable of maintaining at such rated capacity at sub-zero temperatures.

Huang et al. [80] and Lin et al. [76] pointed out that a lithium-ion battery might be able to be discharged normally at low temperatures, but not so during reverse charging process. Nagasubramanian [81] reported that the commercial 18650 lithium-ion battery has only 5% of energy density and 1.25% of power density compared to that obtained at 20°C. Shidore and Bohn [82] summarised the percentage drop in EV range based on three initial temperature conditions (20°C, 0°C and -7°C) during UDDS and UDDSx1.2 aggressive driving cycles. 0%, 9%, and 13% drop in EV range was resulted respectively under UDDS, and 10.7% drop was observed under UDDSx1.2 for an initial temperature of 0°C as compared to 20°C. In addition, capacity fade due to lithium plating upon charging in cold climate has been studied [76, 83]. Zhang et al. [84] made a generalisation that both energy and power of the lithium-ion batteries will be reduced once the temperature falls down to -10°C. Shi et al. [85] conducted an experiment comparing the discharge capacity of the lithium-ion battery used for electric vehicles under both -20°C and 20°C, and showed that 62.6% was obtained at -20°C, smaller than the rated standard.

Poor lithium-ion battery performance under cold climates is therefore studied [84, 86, 87] which can be summarised from four factors: 1) low conductivity of the electrolyte and solid electrolyte interface on the electrode surface [88, 89]; 2) declined solid-state Li diffusivity [80, 84]; 3) high polarisation of the graphite anode [76, 90]; and 4) the sluggish kinetics and transport processes caused by increased charge-transfer resistance on the electrolyte-electrode interfaces [80, 84]. Three contributing factors

of a PHEV lithium-ion battery impact of low ambient temperature at -7°C and 0°C have been quantified [82]. These include limited battery propulsion and regenerative power accounting for 34% of the total reduction in battery power, high battery internal resistance leading to 8-12%, and other losses that attribute to 54-58%. In addition, ten-time increase in resistance has been measured from the commercial 18650-lithium-ion battery at -20°C [91]. Stuart and Hande [92] explained the charging or discharging difficulty at cold temperatures and addressed the concern of potential hazards due to increased charge-transfer resistance. The highly nonlinear overvoltage equivalent resistance (R_{ov}) increases so much at a sufficiently low temperature and SOC making the battery almost unusable. High R_{ov} also causes excessive gassing resulting in a loss of electrolyte, or even case rupturing if the internal pressure generated due to gassing exceeds the capacity of the relief valves. The problems could be solved by formulating [88, 89] or replacing the chemical substances [93, 94] inside the lithium-ion batteries, or seeking for viable battery preheating methods in order to avoid loss in energy and power capability [81, 86] as well as severe battery degradation at sub-zero climates.

3.3. Battery Model Approach

Battery modelling can be defined using a set of equations under specific conditions of interest. The choice of equations, or the mathematical description of batteries, is significant in predicting the behaviour of the system. The thermal behaviour of a lithium-ion battery can be strongly affected by electrochemical and chemical processes occurring inside the cell during charge and discharge [95]. Battery heat generation is complex which requires knowing of how electrochemical reaction rates vary with time and temperature, and how current is distributed, especially within large size batteries. A battery thermal model can be thermal and electrochemical/electrical coupled or decoupled, depending on the heat generation. A fully coupled model uses newly generated parameters for current and potential from the model to calculate the heat generation, so that the temperature distribution in relation with the current and potential can be predicted [96]. The decoupled model may sometimes employ empirical equations based on experimental data. A partially-coupled approach can also be adopted, where the heat generation rate applied at one thermal environment (nonisothermal) was from that obtained previously at a given thermal environment (isothermal model) [97].

3.3.1. Electrochemical/electrical Model

Two categories of the numerical models for obtaining the heat generation will be discussed in this paper: electrochemical model (or first principle model) and equivalent circuit model. The electrochemical model is by far the most used method and is usually a one-dimensional physics-based electrochemical model which has a set of governing equations (Eq. 1-5, Table 6) describing kinetics, transport phenomena and energy dissipation of a cell. It was first developed by Newman's group [98, 99] based on a macro-homogeneous and isothermal model approach [100]. The model (Fig. 7) can be established from two composite electrodes and a separator, along with one-dimensional transport of lithium-ions from the negative electrodes to the positive electrode through the separator. A good agreement with the experimental data performed later by Doyle [101] showed the applicability of such model to almost any of the existing li/lithium-ion systems.

Table 6: Fundamentals of electrochemical model for lithium batteries

Physic Fundamentals	Equations
Electrochemical kinetics	

Reaction rate (Butler-Volmer equation)	$$\bar{j}_{nj} = a_s i_{oj}\left(\exp\left(\frac{\alpha_{aj}F}{RT}\eta_j\right) - \exp\left(-\frac{\alpha_{cj}F}{RT}\eta_j\right)\right) \quad (1)$$ a_s – specific interfacial area of an electrode i_{oj} – exchange current density (a function of lithium concentrations in both electrolyte and solid active materials, $i_{oj} = k(c_e)^{\alpha_{aj}}\left(c_{s,\max} - \bar{c}_{se}\right)^{\alpha_{aj}}\left(\bar{c}_{se}\right)^{\alpha_{cj}}$, where c_e is volume-average lithium concentration in the electrolyte; k is the constant, determined by the initial exchange current density and species concentration) α_{aj}, α_{cj} – anodic and cathodic transfer coefficient of electrode reaction F – Faraday's constant (96,485 C equiv.$^{-1}$) R – universal gas constant T – absolute temperature in Kelvin η_j – local surface overpotential ($\eta_j = \phi_s - \phi_e - U$, where ϕ_s, ϕ_e is volume-average electrical potential in solid phase and electrolyte; U is open circuit potential)
<u>Phase transition & Ion transport</u> **Solid phase conservation of Li^+ species**	$$\frac{\partial}{\partial t}c_s - \frac{D_s}{r^2}\frac{\partial}{\partial r}\left(r^2\frac{\partial}{\partial r}c_s\right) = 0 \quad (2)$$ with boundary conditions $D_s\frac{\partial}{\partial r}c_s\Big\|_{r=0} = 0$, $-D_s\frac{\partial}{\partial r}c_s\Big\|_{r=R_s} = \frac{j^{Li}}{a_s F}$ D_s – mass diffusion coefficient of lithium-ion in the electrolyte r – radial coordinate along active material particle R_s – radius of solid active material particle j^{Li} – transfer current resulting from the lithium insertion/de-insertion at the electrode/electrolyte interface which consumes/generates the species Li^+, $j^{Li} = \begin{cases} a_{s,a}\bar{i}_{n,a} \\ 0 \\ a_{s,c}\bar{i}_{n,c} \end{cases}$ in the cathode, separator and cathode respectively
Electrolyte phase conservation of Li^+ species	$$\frac{\partial}{\partial t}\varepsilon_e c_e - \nabla\cdot\left(D_e^{eff}\nabla c_e\right) - \left(1-t_+^o\right)\frac{j^{Li}}{F} + \frac{i_e\cdot\nabla t_+}{F} = 0 \quad (3)$$ with boundary conditions $\frac{\partial}{\partial x}c_e\Big\|_{x=0} = \frac{\partial}{\partial x}c_e\Big\|_{x=L} = 0$ for 1D analysis ε_e – volume fraction/porosity of electrolyte D_e^{eff} - effective diffusion coefficient (Bruggeman relation, $D_e^{eff} = D_e\varepsilon_e^{1.5}$)

	t_+^o - transference number of the Li^+ with respect to the velocity of solvent (a function of electrolyte concentration, if assuming constant, $\frac{i_e \cdot \nabla t_+}{F}$=0)
Energy dissipation **Charge conservation in the solid phase**	$$\nabla \cdot \left(\sigma^{eff} \nabla \phi_s\right) - j^{Li} = 0 \quad (4)$$ with boundary conditions $-\sigma_-^{eff} \frac{\partial}{\partial x}\phi_s\Big\|_{x=0} = \sigma_+^{eff} \frac{\partial}{\partial x}\phi_s\Big\|_{x=L} = \frac{I}{A}$, $\frac{\partial}{\partial x}\phi_s\Big\|_{x=\delta_-} = \frac{\partial}{\partial x}\phi_s\Big\|_{x=L-\delta+} = 0$ for 1D analysis σ^{eff} – effective conductivity of the solid phase
Charge conservation in the electrolyte	$$\nabla \cdot \left(k^{eff} \nabla \phi_e\right) + \nabla \cdot \left(k_D^{eff} \nabla \ln c_e\right) + j^{Li} = 0 \quad (5)$$ with boundary conditions $\frac{\partial}{\partial x}\phi_e\Big\|_{x=0} = \frac{\partial}{\partial x}\phi_e\Big\|_{x=L} = 0$ for 1D analysis k^{eff} – diffusional conductivity (Bruggeman relation, $k^{eff} = k\varepsilon_e^{1.5}$) k_D^{eff} – effective ionic conductivity ($k_D^{eff} = \frac{2RTk^{eff}}{F}\left(t_+^o - 1\right)\left(1 + \frac{d \ln f_\pm}{d \ln c_e}\right)$, where $f_\pm$ is molecular activity coefficient of the electrolyte)

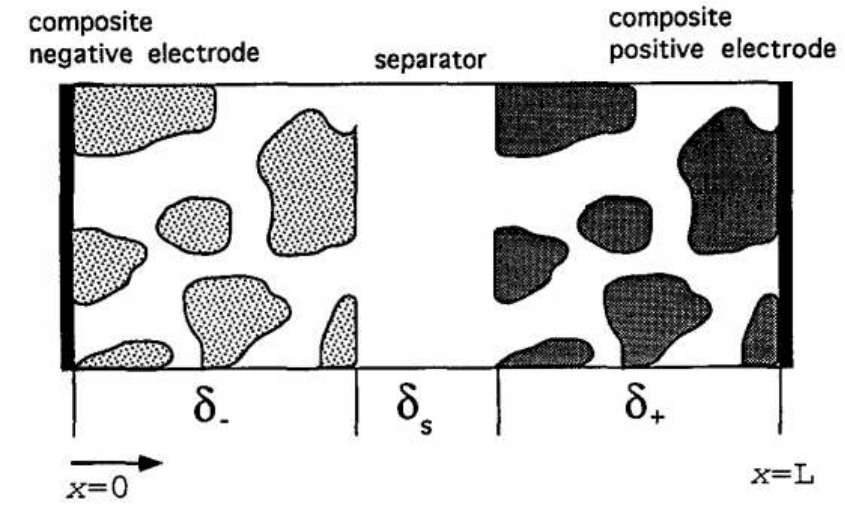

Figure 7: Dual lithium-ion insertion cell sandwich structure developed by [99].

The equivalent circuit model, which does not consider the physical fundamentals of the battery cells, provides a simple structure to capture the input/output relationship of the battery. It utilises common

electrical components such as resistors, capacitors, and voltage sources to form a circuit network [102]. Typical equivalent circuit models used for vehicle batteries are Rint model (or Internal Resistance model), Resistance Capacitance (RC) model, Thevenin model, and PNGV (Partnership for New Generation of Vehicles) model [102-108]. Rint model (Fig. 8 (a)) assumes that the battery is an ideal voltage source in series with the resistance. RC model (Fig. 8 (b)) was developed by SAFT Battery Company containing capacitors within the branches of the circuit to show more close-to-real battery characteristics. A one or two RC block model without parasitic branch is generally accepted for lithium cells according to [107]. In addition, Thevenin model (Fig. 8 (c)) has been widely used in early battery management system and was developed based on Rint model which connects a parallel RC network in series and takes into account of polarisation. Finally, the PNGV model (Fig. 8 (d)) was modified from Thevenin model with a slight increase in circuit elements (a capacitor $1/U'_{oc}$ in series is added) [108]. Table 7 summarises basic equations for those models.

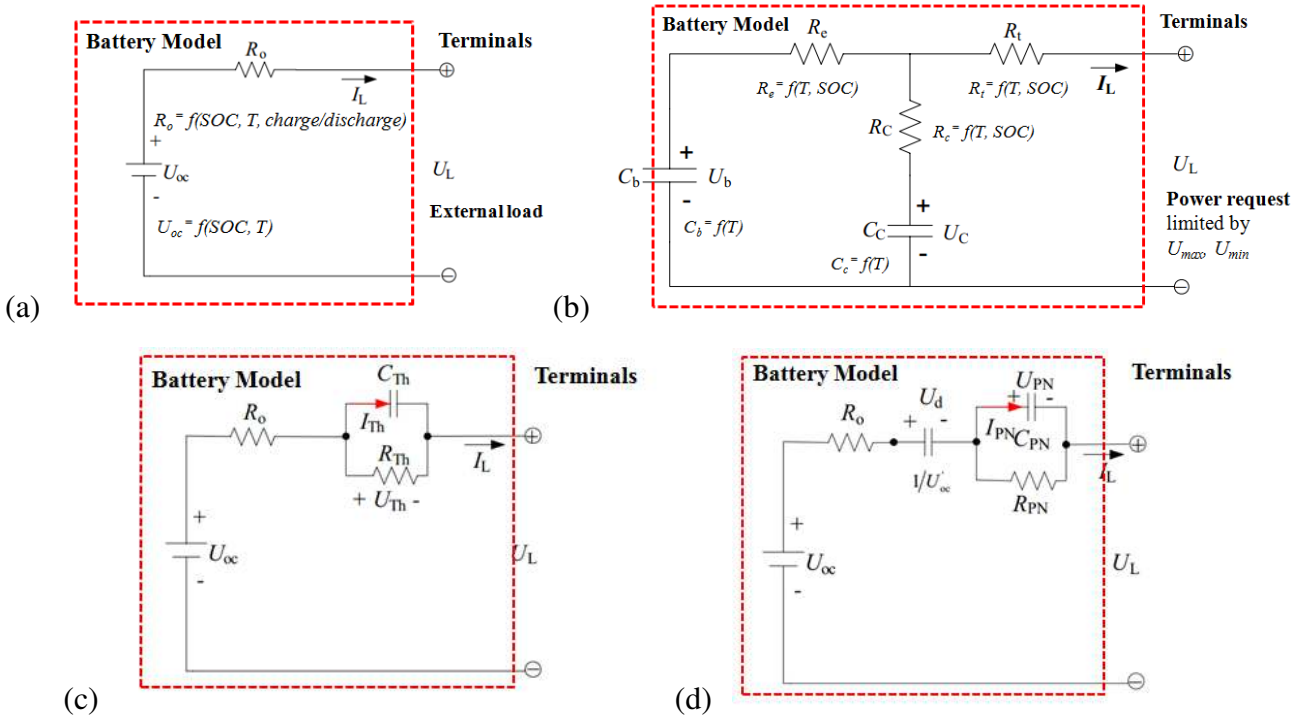

Figure 8: Various equivalent circuit models used for vehicle batteries (modified from [102, 103, 105]: (a) Rint model; (b) RC model; (c) Thevenin model; and (d) PNGV model.

Table 7: Equations of electrical model for lithium batteries

Model	Equations
Rint Model (internal resistance model)	$U_L = U_{oc} - I_L R_o$ (6) U_L – terminal voltage U_{oc} – open-circuit voltage I_L – load current (+ discharge, - charging)

	R_o – internal resistance or ohmic resistance
RC Model	$$\begin{bmatrix}\dot{U}_b \\ \dot{U}_c\end{bmatrix}=\begin{bmatrix}\frac{-1}{C_b(R_e+R_c)} & \frac{1}{C_b(R_e+R_c)} \\ \frac{1}{C_c(R_e+R_c)} & \frac{-1}{C_c(R_e+R_c)}\end{bmatrix}\begin{bmatrix}U_b \\ U_c\end{bmatrix}+\begin{bmatrix}\frac{-R_c}{C_b(R_e+R_c)} \\ \frac{-R_e}{C_c(R_e+R_c)}\end{bmatrix}[I_L] \quad (7)$$ $$[U_L]=\begin{bmatrix}\frac{R_c}{R_e+R_c} & \frac{R_e}{R_e+R_c}\end{bmatrix}\begin{bmatrix}U_b \\ U_c\end{bmatrix}-\left[R_t+\frac{R_eR_c}{R_e+R_c}\right][I_L] \quad (8)$$ C_c – surface capacitor (small capacitance which mainly represents the surface effects of a battery) C_b – bulk capacitor (large capacitance which represents the ample capability of a battery to store charge) U_b, U_c – voltages across capacitor C_b and C_c R_t – terminal resistance R_e – end resistance R_c – capacitor resistance
Thevenin Model	$$\dot{U}_{Th}=-\frac{U_{Th}}{R_{Th}C_{Th}}+\frac{I_L}{C_{Th}} \quad (9)$$ $$U_L=U_{OC}-U_{Th}-I_LR_o \quad (10)$$ C_{Th} – equivalent capacitance that reflects the transient response during charge and discharge U_{Th} – voltage across C_{Th} R_{Th} – polarization resistance I_{Th} – outflow current
PNGV Model	$$\dot{U}_d=U'_{oc}\,I_L \quad (11)$$ $$\dot{U}_{PN}=-\frac{U_{PN}}{R_{PN}C_{PN}}+\frac{I_L}{C_{PN}} \quad (12)$$ $$U_L=U_{oc}-U_d-U_{PN}-I_LR_o \quad (13)$$ U_d, U_{PN} – voltages across $1/U'_{oc}$ and C_{PN} I_{PN} – outflow current of C_{PN}

Many studies extended the one-dimensional electrochemical model to include an energy balance to capture temperature within the cell. Gu and Wang [96] demonstrated a diagram (Fig. 9) of thermal-electrochemical coupled modelling approach and the coupled model takes into account of multi-scale physics in lithium-ion battery including kinetics (electrochemical kinetics), phase transition (solid-phase lithium transport), ion transport (lithium transport in electrolyte), energy dissipation (charge conservation/transport), and heat transfer (thermal energy conservation). Fig. 10 illustrates such micro-

macroscopic modelling approach applied into a lithium-ion vehicle battery. Moreover, an example of a thermal-electrical coupled model used for an A123 $LiPO_4$/graphite battery is demonstrated in Fig. 11. A control-oriented model block is used to form the coupled model and it can be built from two subsystems namely equivalent circuit models and thermal models with parameter estimation linked in between for real time implementation.

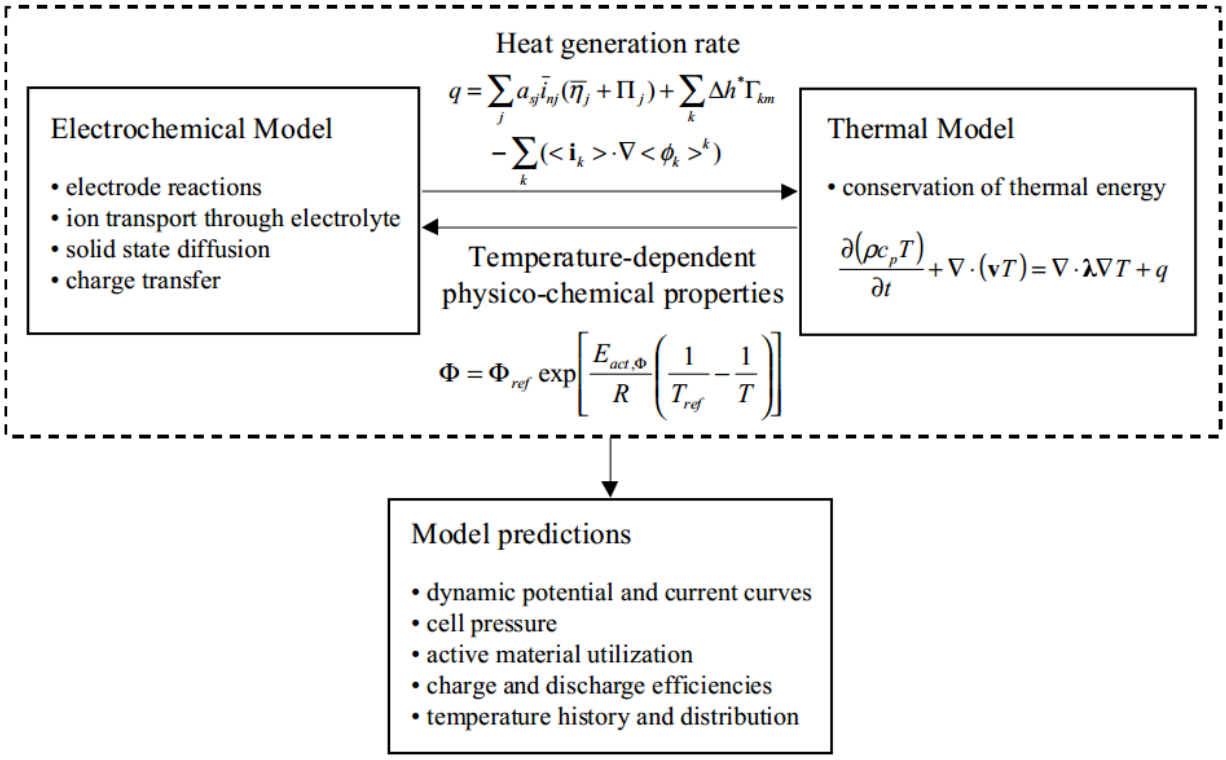

Figure 9: Thermal-electrochemical coupled modelling approach [96].

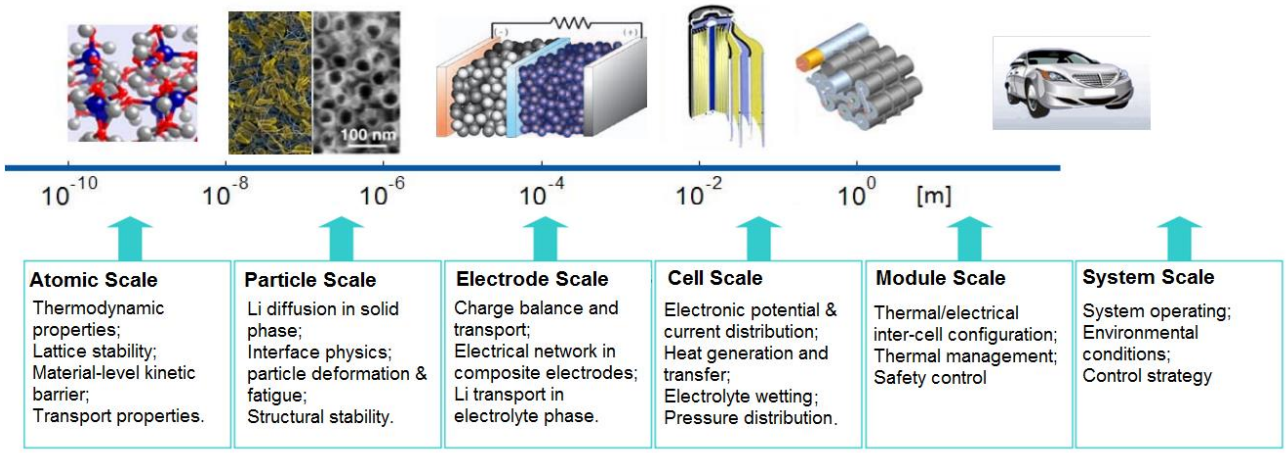

Figure 10: Multi-scale physics and micro-macroscopic modelling approach applied into a lithium-ion battery (modified from [109, 110]).

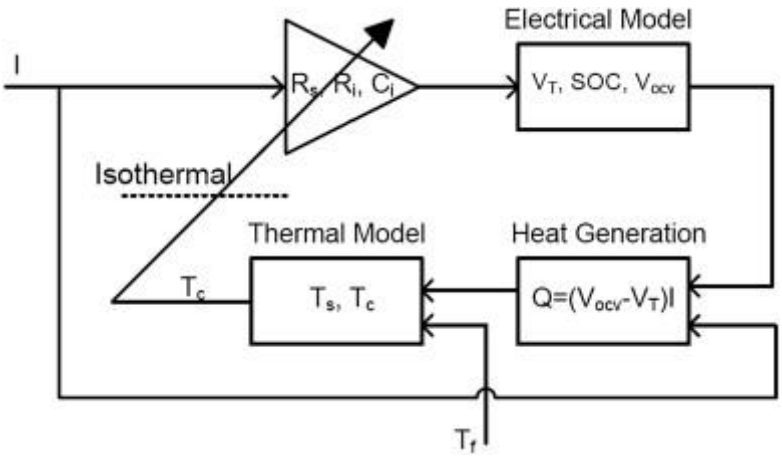

Figure 11: Coupled thermal-electrical model for an A123 LiPO4/graphite battery [111].

3.3.2. Thermal Model and Heat Generation Modelling

The battery thermal model accounts for heat accumulation, convection, conduction and heat generation (Eq. 14, Table 8). To note, the term $\rho c_p v \cdot \nabla T$, i.e. the convective heat transfer inside the battery, is always neglected because liquid electrolytes in a lithium-ion battery tend to show limited mobility. Another commonly used method is called lumped thermal model, which balances accumulation, convective heat dissipation to the surroundings, and heat generation (Eq. 15, Table 8). By assuming the battery as a lumped body, the temperature of the battery is considered to be uniformly distributed in all directions at all times during the transient heat transfer. This often applies to the condition where single cells have small thickness so that the Biot number ($Bi = \frac{hL}{\lambda} << 1$) is less than 1.

Battery heat is generated due to activation, concentration and ohmic losses [112]. Various equations have been applied to calculate the heat generation rate in lithium-ion batteries. The local heat generation (Eq. 16, Table 8) has shown to be more accurate but is very complex. Bernardi et al. [113] formulated the thermodynamic energy balance on a single cell, and a simplified form (Eq. 17, Table 8) has been readily accepted in small lithium-ion batteries if assuming no heat from mixing or phase change, uniform temperature or SOC, and only one electrochemical reaction takes place [96]. This equation can be used if the experimental over-potential and entropic heat coefficients are known. Attempts to experimentally examine the irreversible electrochemical heat generation for lithium-ion batteries can be obtained from two methods: accelerated-rate calorimetry (ARC) and isothermal heat conduction calorimetry (IHC) [112]. The ARC method allows the heat generation rate to be calculated based on an energy balance between the battery (heat source) and a constant temperature sink. The IHC method maintains the battery at a constant temperature throughout the whole operation and uses high-accuracy thermopiles attached to the surface of the battery to measure the heat rate. For reversible heat, the most common way is to measure the open-circuit potential (OCP) variation with temperature at a constant SOC. However, studies that used the aforementioned experimental methods have only been investigated where the total heat generation was obtained under currents no greater than 2C, and many were carried out under ambient temperature of 20°C or 25°C. Temperature influence was always omitted or for those who investigated it, the chosen temperature range was small. According to Hong et al. [114], small temperature changes cause significant heat accumulation, greater than the heat rejection of the device in some cases. Moreover, Sato [115] analysed the thermal behaviour of lithium-ion batteries (Sony 18650 cell) and developed a heat intake and release model (Eq. 18-19, Table 8).

The heat generation equations which constitute reaction heat Q_r, polarisation heat Q_p, and Joule heat Q_j during charging and discharging have been established and the obtained results (used a constant R_t at 50% DOD) agreed well with experiment.

Table 8: Summary of thermal model equations

Heat Transfer and Energy Balance	
Battery thermal model	$$\rho c_p\left(\frac{\partial T}{\partial t}+v\cdot\nabla T\right)\approx\frac{\partial\left(\rho c_p T\right)}{\partial t}=\nabla\cdot\lambda\nabla T+q \quad (14)$$ ρ – composite/average density of the battery c_p – composite/average heat capacity per unit mass under constant pressure v – velocity of the electrolyte λ – composite/average thermal conductivity in x, y, z direction q – heat generation
Lumped thermal model	$$\frac{d\left(\rho c_p T\right)}{dt}=hA_s\left(T-T_\infty\right)+q \quad (15)$$ h – heat transfer coefficient for forced convection from each cell A_s – cell surface area exposed to the convective cooling medium T – free stream temperature of the cooling medium
Heat Generation Modelling	
Local heat generation *(can be linked with electrochemical model)*	$$q=a_{sj}i_{nj}\left(\phi_s-\phi_e-U_j\right)+a_{sj}i_{nj}\left(T\frac{\partial U_j}{\partial T}\right)+\sigma^{eff}\nabla\phi_s\cdot\nabla\phi_s+k^{eff}\nabla\phi_e\cdot\nabla\phi_e+k_D^{eff}\nabla\ln c_e\cdot\nabla\phi_e \quad (16)$$ 1st term: irreversible heat 2nd term: entropic effect (i.e. reversible heat) 3rd: ohmic heat arising from the solid phase 4th & 5th term: ohmic heats in the electrolyte phase
Simplified heat generation *(obtained from experiment, in commonly use)*	$$q=I\left(U_{OC}-V\right)-I\left(T\frac{dU_{OC}}{dT}\right) \quad (17)$$ 1st term: joule heating 2nd term: entropy change I – discharge current density U_{OC} – open circuit potential V – cell voltage

Heat generation (*Sato [115]*)	$$Q_{charge} = -3.37 \times 10^{-2} Q_1 I_c + 3.60 R_{t,c} I_c^2 \quad (18)$$ $$Q_{discharge} = 3.37 \times 10^{-2} Q_1 I_d + 3.60 R_{t,d} I_d^2 \quad (19)$$ Q_r – reaction heat, $Q_r = -3.37 \times 10^{-2} Q_1 I$ Q_p – polarisation heat, $Q_p = 3.60 R_p I^2$ Q_j – joule heat, $Q_j = 3.60 R_e I^2$ Q_1 – heat generated (kJ/mol) from positive electrode ($LiCoO_2 \rightarrow Li_{1-x}CoO_2 + xLi^+ + xe^-$) and negative electrode ($C + xLi^+ + xe^- \rightarrow CLi_x$) I_c, I_d– battery charge/discharge current R_p – resistance due to polarisation R_e – internal resistance $R_{t.c}$, $R_{t.d}$ – total electrical resistance during charging/discharging

3.3.3. Coupled and Decoupled Models

A summary of the coupled thermal-electrochemical models used in literature is provided in Table 9. Arrhenius law (Eq. 20) can be applied to mass transport and kinetic parameter ψ to couple electrochemical and thermal models. Significantly, the lumped thermal model used by [97, 116-118] that neglects spatial temperature variation by assuming the temperature is uniform all over the cell (small Biot number, Bi<<1) may result in an error of 15% in total thermal energy under higher discharge rates [119] (Fig. 12). The local heat generation method performed by [116, 117, 119-122] has shown to be more accurate. Srinivasan and Wang [119] plotted the heat generated due to various factors contributing to the total heat (Fig. 13). They pointed out that the reversible heating effect can be important at low discharge rates (0.01-1C) (Fig. 13 (a)), but will be dominated by irreversible (reaction and ohmic) heating at high discharge rates (1-10C) (Fig. 13 (b)). Furthermore, 2D thermal model has been used in most studies because a larger aspect ratio of the cell is available. The need for a 2D model can only be reduced if the cell has a smaller aspect ratio or the current collectors have increased thickness with two orders of magnitude larger thermal conductivity [119].

$$\psi = \psi_{ref} \exp\left(\frac{E_{act}^{\psi}}{R}\left(\frac{1}{T_{ref}} - \frac{1}{T}\right)\right) \quad (20)$$

ψ_{ref} – property value defined at reference temperature T_{ref}
E_{act}^{ψ} - activation energy which controls the temperature sensitivity of each individual property ψ

Table 9. Summary of thermal-electrochemical models used in literature

Refs.	Battery type (positive/negative electrode)	Configuration	Electrochemical model (ECM)	Thermal model (Eq. from Table 8)
Pals and Newman [97]	$LiPEO_8$-$LiCF_3SO_3$/$LiTiS_2$	Small cell	1D ECM developed by Doyle et al. [98]	Eq. 15, Eq. 17
Song and Evan [120]	$LiMn_2O_4$/graphite	Prismatic		Eq. 14, Eq. 17 (2D)
Gu and Wang [122]	$LiMn_2O_4$/graphite	Large size lithium-ion cell for HEV/EV applications		Eq. 14, Eq. 16
Gomadam et al. [121]	$LiCoO_2$/graphite	Prismatic		Eq. 14, Eq. 16
Srinivasan and Wang [119]	$LiMn_2O_4$/graphite	Small cell		Eq. 14, Eq. 16 (2D)
Smith and Wang [116]	$LiCoO_2$/graphite	72 cell battery pack		Eq. 15, Eq. 16 *(neglected reversible heating)*
Kim and Smith [109, 123]	$LiMn_2O_4$/graphite	Cylindrical		Eq. 14 (2D)
Fang et al. [117]	NMC/graphite	Cylindrical		Eq. 15, Eq. 16 *(neglected reversible heating)*
Lee et al. [110]	$LiMn_2O_4$/graphite	Cylindrical		Eq. 14 (3D)
Cai and White [124]	$LiFePO_4$/graphite	/		Eq. 14, Eq. 16
Prada et al. [118]	$LiFePO_4$/graphite	Cylindrical		Eq. 15, Eq. 17
Baker and Verbrugge [125]	$LiMn_2O_4$/graphite	Thin film	2D	Eq. 14, Eq. 17 (2D)

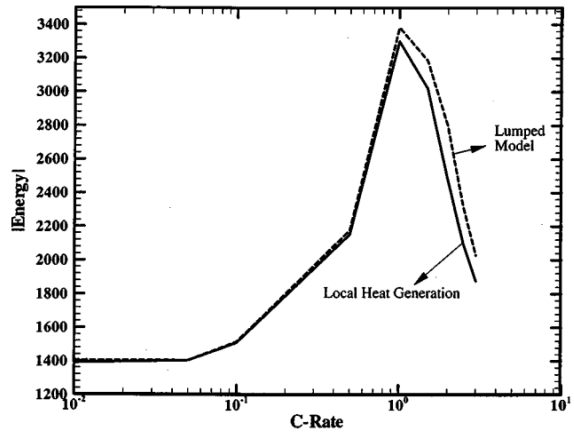

Figure 12: A comparison of thermal energy generated using local heat generation and lumped thermal models under adiabatic conditions [119].

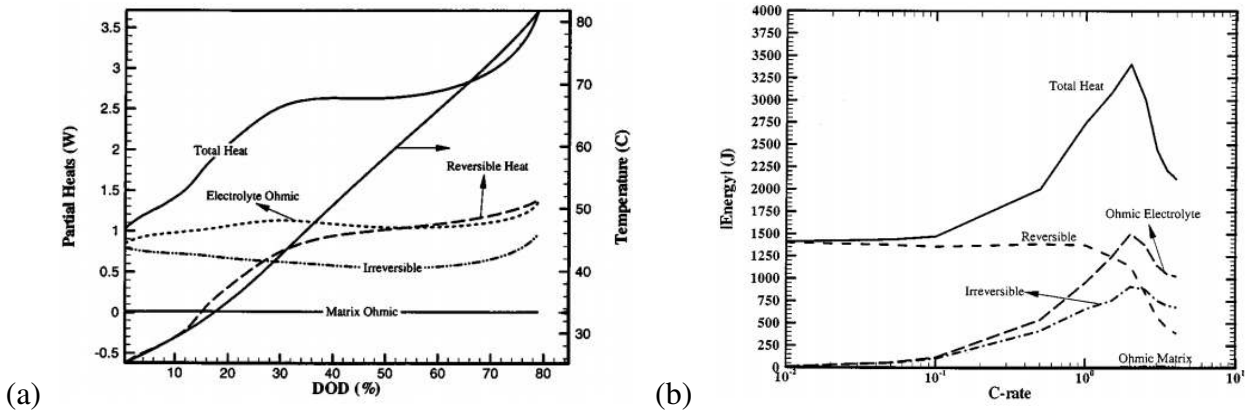

Figure 13: Heat generated due to various terms contributing to the total heat (a) under 2C discharge of a lithium-ion cell; and (b) under various discharge C rates [119].

For large-scale battery pack applied in HEVs and EVs, the collective thermal effects of electrochemical process are normally obtained from experiment measurements and therefore treating such battery pack as the heat source in a standalone thermal model is possible [126]. Examples are shown in Table 10, which established 1-3D decoupled thermal models where the heat generation was obtained from experiment. For such thermal model development, the heat is assumed to be generated within the solid domain (conductive heat transfer) and then be transferred to the surrounding medium at boundary surfaces (convection and radiation) (Fig. 14). Four assumptions can be made to estimate the battery thermal behaviour: 1) homogenous internal cell condition; 2) uniform temperature distribution of internal heat source; 3) no convection or thermal radiation exists inside the battery cell; 4) thermophysical properties are independent of temperature. However, the necessity of decoupling needs to be justified since discrepancies in predicting battery cell temperature can be found between thermo-electrochemical coupled and decoupled model. As reported by Gu and Wang [96], no temperature difference was detected under 1C charging and two convective heat transfer conditions (5, 25W/m^{2}K), but discrepancies were noted under 1.5V float charging, especially at high percentage of normal cell capacity (Fig. 15).

Table 10. Standalone thermal models (decoupled) developed in various studies

Refs.	Battery type (positive/negative electrode)	Configuration	Thermal Model	Heat generation method
Chen and Evans [127]	LiV_6O_{13}/Li	Prismatic	2D	ED
Chen and Evans [128]	$LiTiS_2$/Li	Prismatic	3D	ED
Chen and Evans [129]	$LiCoO_2$/graphite	Prismatic	2D	ED
Hallaj et al. [130, 131]	$LiCoO_2$/graphite	Cylindrical	1D	ARC
Chen et al. [132]	$LiCoO_2$/graphite	Cylindrical	3D	ED
Onda et al. [133]	$LiCoO_2$/graphite	Cylindrical	1D	OCP
Chen et al. [134]	$LiCoO_2$/graphite	Cylindrical	2D	ED

Kim et al. [135, 136]	$LiNiCoMnO_2$ /graphite	Prismatic	2D	ED
Taheri et al. [126]	$Li[NiC_oMn_2]O_2$ /graphtie	Prismatic	3D	ED

Note: ED – Experimental data (such as over-potential and entropic heat coefficients to predict the heat generation rate); ARC – accelerated rate calorimeter; OCP – open-circuit potential;

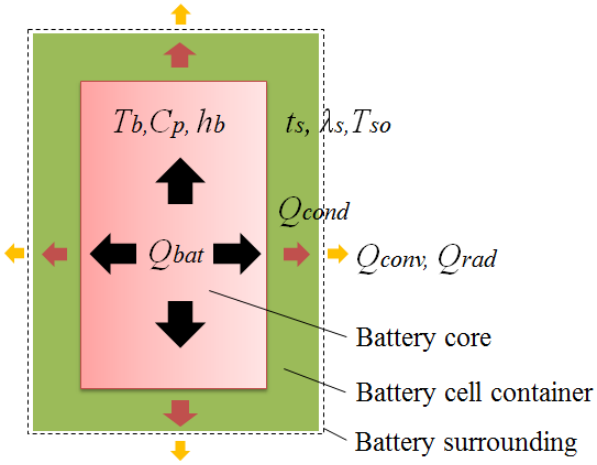

Figure 14: Heat transfer from internal battery cell to the cell container surface and to the surroundings.

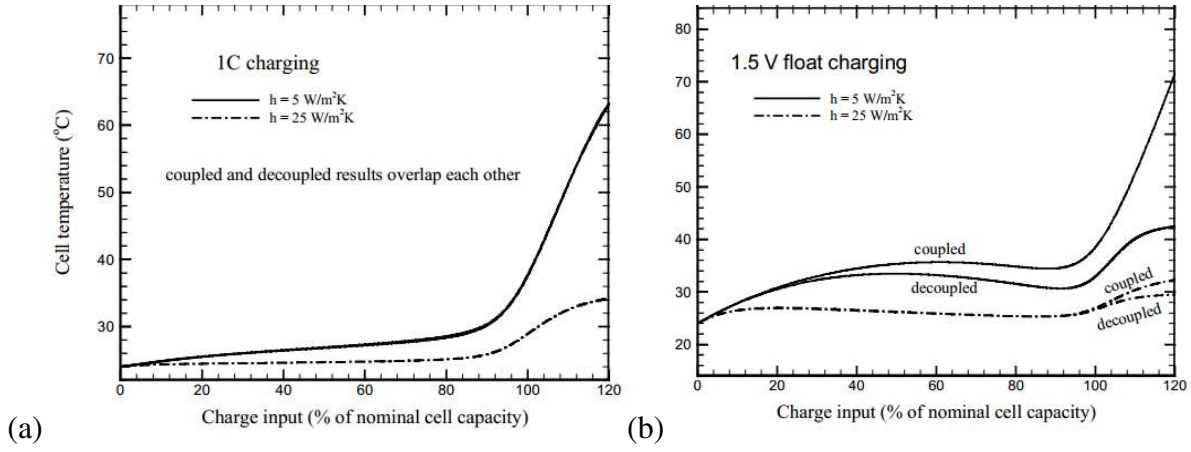

Figure 15: Comparison of predicted cell temperature between thermo-electrochemical coupled and decoupled model during (a) 1C charging and (b) 1.5V float charging [96].

4. Battery Thermal Management Strategies

4.1. Design Considerations

Temperature effects, heat sources and sinks, EV/HEV batteries, and temperature control should be considered before designing a good battery thermal management (Fig. 16). Either low (<15°C) or high temperature (>50°C) will progressively reduce the cycle life, and the threat of thermal runaway at a

temperature higher than 70°C leads to cell failure. Pesaran [137] benchmarked the operating temperature for a variety of batteries including lead-acid, NiMH, and lithium-ion. He pointed out that the suitable range should be between 25°C to 40°C with a maximum of 5°C difference from module to module. He [138] later on demonstrated the temperature impact on life, safety and performance of lithium-ion batteries (Fig. 17) and suggested a range of 15-35°C as desired working temperature. Ladrech [139] also provided a temperature band for lithium-ion batteries obtained from suppliers and divided the range into four sections namely decline of battery capacity and pulse performance (0-10°C), optimal range (20-30°C), faster self-discharge (30-40°C), and irreversible reactions and short-circuit (40-60°C). According to Sato [115], charging efficiency and life cycle can be significantly reduced if the battery temperature exceeds 50°C. Khateeb et al. [140] showed that the thermal runaway of the lithium-ion cells initiates at the temperature range of 70-100°C jeopardising battery safety. Moreover, Lu et al. [141] made a detailed summary of stages that progress to thermal runaway and stated that the SEI breakdown starts at 80°C. These works all imply that the maximum working temperature for lithium-ion batteries should be kept below 40°C; and the minimum, above 15°C.

The heat sources and sinks can be identified from the effects of internal impedance and chemical reactions during charge or discharge. Precautions should be taken to avoid unexpected overheating or temperature rise that leads to cell failure. The cooling/heating methods available for EV and HEV batteries, in addition, are required to be considered separately as EV battery is more subject to low temperature rise, whereas HEV battery is likely to encounter high temperature rise. Fig. 18 explains the thermal problems EV and HEV will face by comparing them at the same battery handling power. EV operates at a deep discharge rate (1C) while HEV tends to operate at a very high rate (10C). As a result, EV battery may still need to be heated up at low temperature while HEV can have overheating problem even though they both dissipate the same amount of heat.

Two major problems caused by temperature can be found when it comes to battery cooling: 1) the temperature exceeds permissible levels during charge or discharge; and 2) uneven temperature distribution attributes to a localised deterioration [142]. Effective battery cooling should be able to maintain the allowed maximum cell temperature, reduce the temperature difference between cells, and ensure the cell being operated under the optimal working temperature range [143, 144]. Viable battery preheating methods, in addition, are required to eliminate loss in energy and power capability [81, 86] as well as severe battery degradation under sub-zero climates. The battery preheating system must be equipped with an ultimate energy optimisation, which provides an efficient and flexible solution in maximising the operating range without jeopardising cabin comfort and battery performance. The system must function well in driving, charging and long term parking.

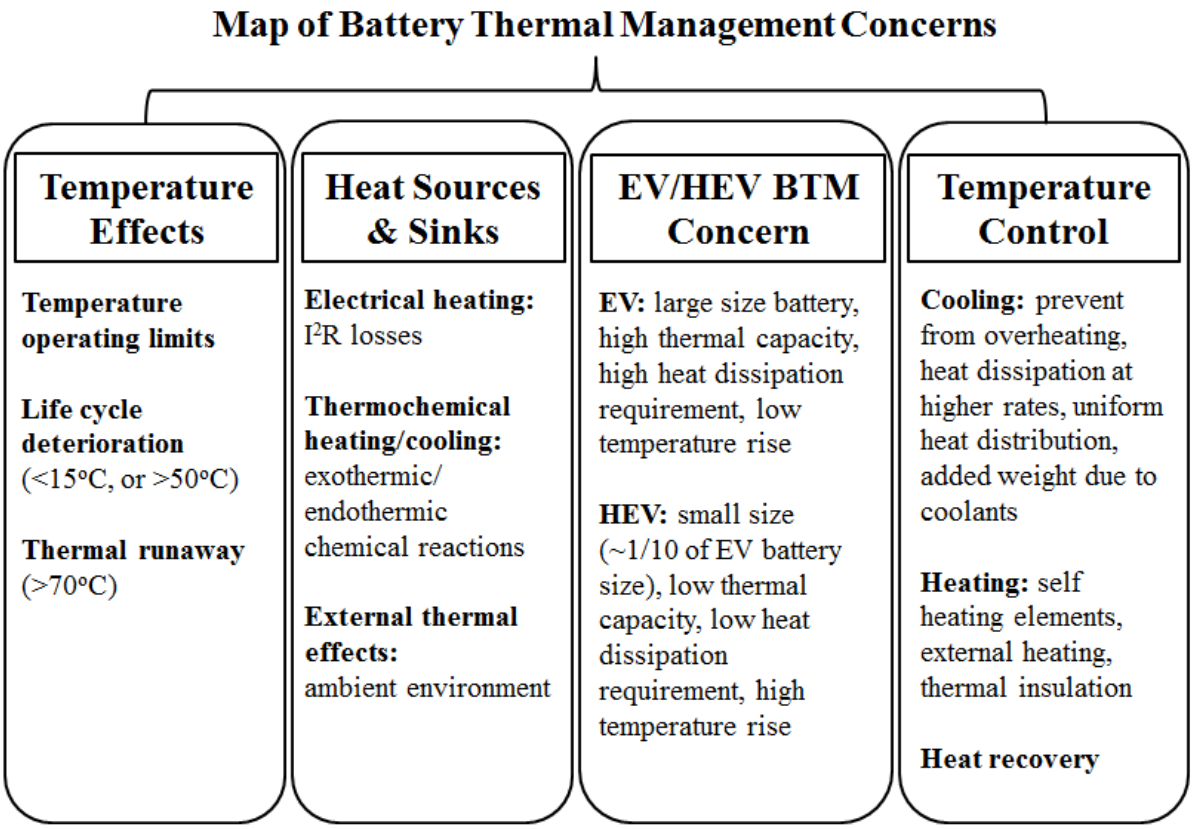

Figure 16: Battery thermal management mapping

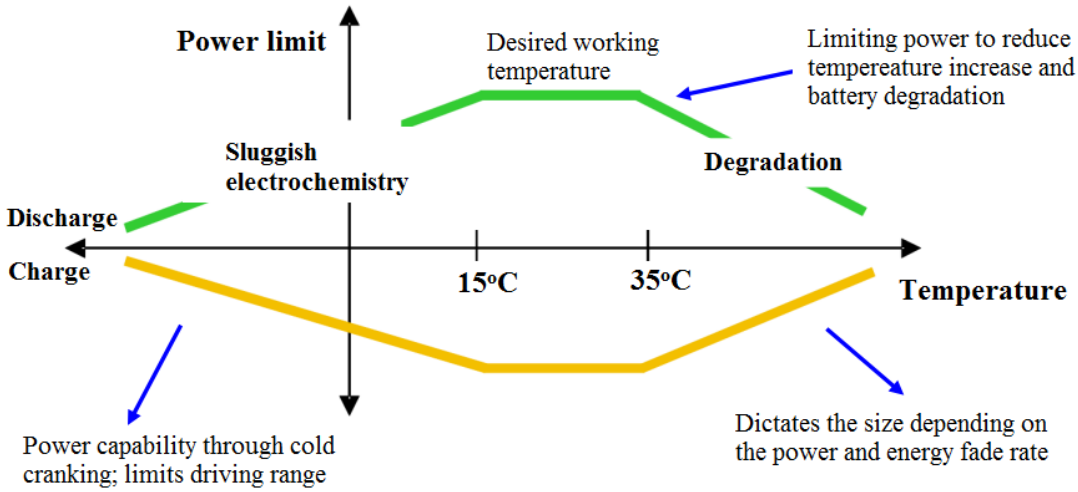

Figure 17: Temperature impact on life, safety and performance of lithium-ion batteries [138].

Table 11: Suggested operating temperature range for lithium-ion batteries

Ref (s)	Advised Temperature Range for optimal performance (°C)	Battery type
Sato [115]	<50	Lithium-ion
Pesaran [137]	25-40	Lead-acid, NiMH, and Lithium-ion
Panasonic [145]	0-45 for charge -10-60 for discharge	Lithium-ion
Ladrech [139]	20-30	Lithium-ion
Pesaran et al. [138]	15-35	Lithium-ion

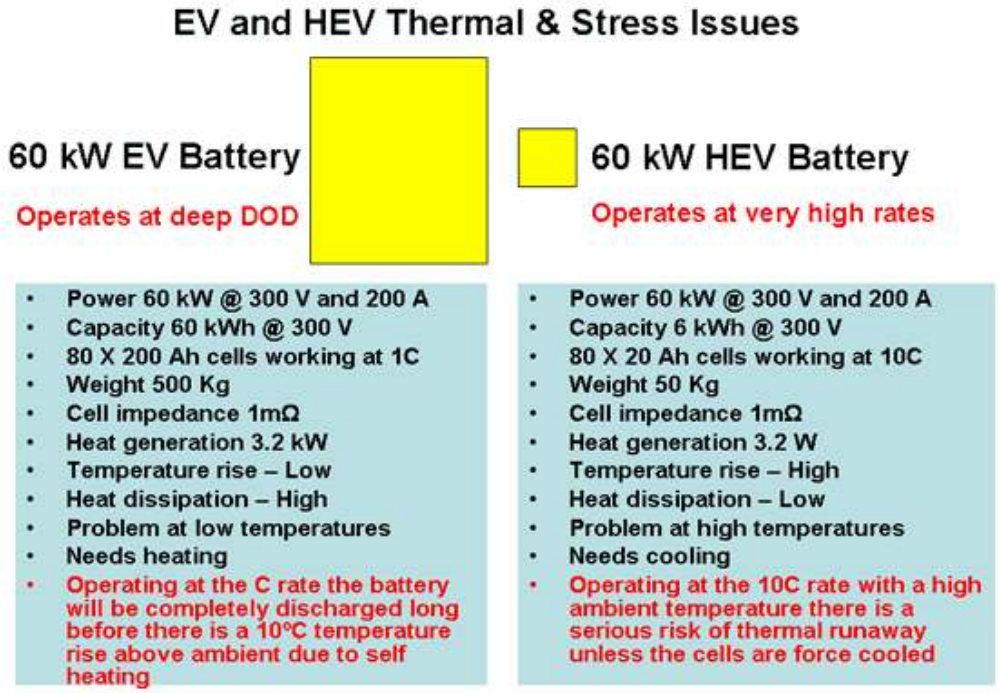

Figure 18: EV and HEV thermal & stress issues [146]

4.2. Thermal Management Strategies

Battery thermal management (BTM) is therefore required to help the battery operate at a desirable working temperature range at all times preventing battery degradation [147, 148], thermal runaway [149-151], and dropped discharge capacity due to sub-zero climate [76]. The thermal management strategies can be either internal or external. Internal cooling as an alternative to allow heat to be removed directly from the source without having to be rejected through the battery surface has been investigated yet scarce. Choi and Yao [152] suggested using forced circulation of the electrolyte in lead-acid batteries to improve heat removal and cell temperature uniformity but it was not practical for lithium-ion batteries. Parise [153] came up with the idea of using thermoelectric coolers in lead-acid cell partitions and/or between positive-negative plate pairs where the heat was produced. A recent study conducted by Bandhauer and Garimella [154] introduced microchannel phase change internal cooling concept to improve thermal gradients and temperature uniformity in a commercially available

C/$LiFePO_4$ lithium-ion batteries. The microchannels were incorporated in either a thick current collector or into a sheet of inert material which was placed in between a split current collector. Internal battery preheating, in addition, involves the use of self-internal heating and mutual pulse heating [87], or alternating current (AC) heating [92]. It is recognised that the internal BTM for lithium-ion batteries is limited and should be further explored due to the potential for higher temperature uniformity both within an individual cell and among cells in a pack.

BTM external to the batteries will be discussed extensively in this paper. It can be categorised into passive (only the ambient environment is used) or active (a built-in source provides heating and/or cooling), or based on medium [10, 142, 155]: 1) air for cooling/heating/ventilation; 2) liquid for cooling/heating; 3) phase change materials (PCM); 4) heat pipe for cooling/heating; and 5) combination of 1)-4).

4.2.1. Air

Either natural or forced air convection can be used for air BTM. Fig. 19 illustrates three air BTM methods including passive air cooling, passive air cooling/heating and active air cooling/heating. Choi and Yao [156] investigated lead-acid batteries and advised the difficulty in sufficiently mitigating the temperature either by natural or forced air convection. Chen and Evans [127] argued that neither passive nor active air cooling can efficiently dissipate heat in large-scale batteries, and Pesaran et al. [157] found out that air cooling is adequate for parallel HEVs but not for EVs and series HEVs. Kim and Persaran [158] claimed that passive air cooling is possible for batteries of low energy density, but for batteries of high energy density such as lithium-ion batteries, an active air system is required. Large thermal gradients between the cell centre and the battery pack boundary can be resulted if no active air thermal management is provided. Those thermal gradients lead to unequal charge or discharge capacity of the battery cell, hence a proper active air cooling device to obtain an optimal battery performance is necessary. Increasing the heat transfer coefficient of the surrounding air by forced air cooling is critical, in spite of design complexity and additional power requirements.

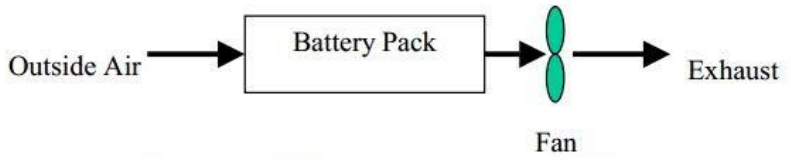

(a) Passive air cooling

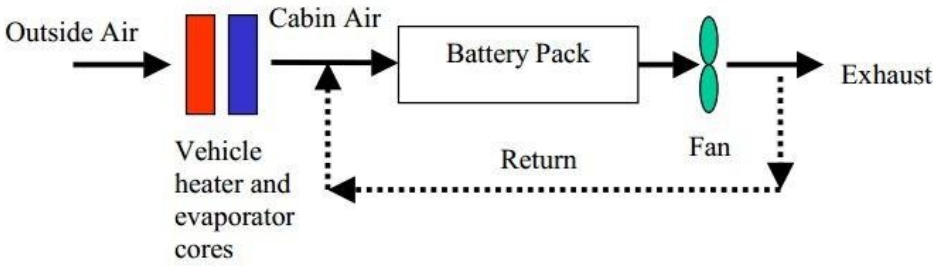

(b) Passive air cooling/heating

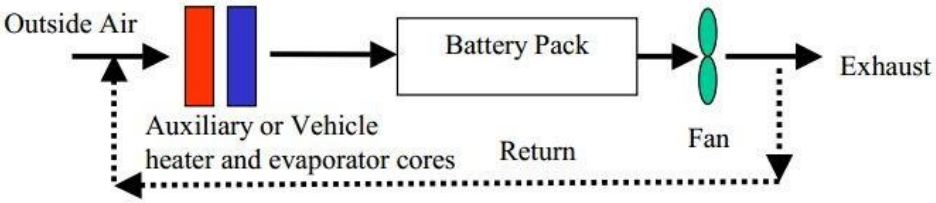

(c) Active air cooling/heating

Figure 19: Air BTM methods [159].

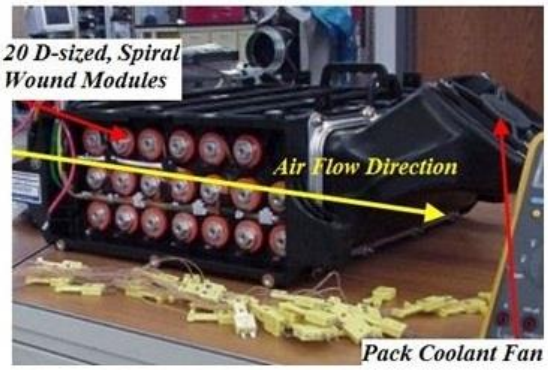

(a) Insight pack

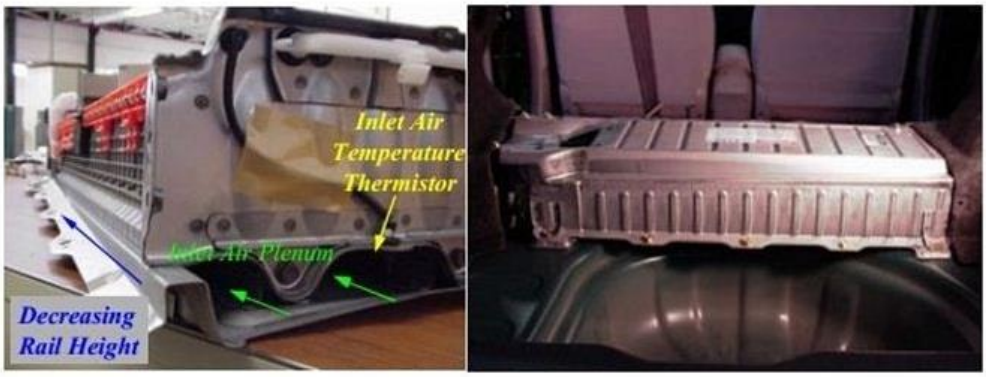

(b) Prius pack

(c) Highlander pack

Figure 20: (a) Insight pack [160]; (b) Prius pack [161]; and (c) Highlander pack [162] using air BTM.

There are two ways that an active air BTM adopts [163]. One is to take the air directly from air-conditioned vehicle cabin to either cool or heat the battery. The other is to utilise the treated air from a secondary loop which consists of a separate micro air conditioning unit. Both methods consume relatively large proportion of space for air ducts, blower and/or air conditioning unit, and add a substantial amount of weight to the whole system. Despite the fact that the latter is much more complex and costly, it performs better by using independent/pre-treated air to cool or heat the battery.

The 2000 Honda Insight [160, 164], 2001 Toyota Prius [160, 161, 164], and Toyota Highlander [162] utilise conditioned air taken from the cabin and exhausted to the ambient. Each battery pack (NiMH batteries) has unique module arrangement to mitigate temperature mal-distribution across the cells. Insight pack (Fig. 20 (a)) has a configuration similar to an aligned tube-bank and employs a small 'muffin' fan to force air convection between modules. Prius pack (Fig. 20 (b)) uses a parallel air flow scheme and the air is drawn by a 12-volt blower installed above the driver's side rear tire well. The Highlander pack (Fig. 20 (c)), in addition, which is installed with three fans for separate module units help eliminate efficiency loss due to excessive heat. In the test conducted on Prius pack, the observed thermal gradient was 4-8.3ºC dependent on the blower speed and ambient temperature [161]. The surface temperature was monitored in a few discrete locations so the true maximum temperature differential was unknown. However, it is clear that air is not the best heat transfer medium to maintain excellent temperature uniformity for lithium-ion battery packs, which have more inherent safety risks than NiMH battery packs [10].

Improvements towards air BTM have been performed but with encountered difficulties. Nelson et al. [165] discussed that air cooling method was ineffective to cool the battery down to 52°C if initial battery temperature was higher than 66°C. Lou [166] designed a cinquefoil battery pack for NiMH batteries with aim of heat transfer enhancement. For such air thermal control method, making the temperature difference below 5°C seemed to be impossible and a high degree of temperature uniformity could be resulted between the location near and away from the fan. More recently, Mahamud and Park [144] proposed a reciprocating method in order to create a much uniform temperature profile mitigating the temperature gradient and this has been proven to be better than conventional unidirectional air cooling.

4.2.2. Liquid

As opposed to air, liquid has higher thermal conductivity and heat capacity, and liquid BTM is regarded as a better solution; can be divided into passive or active methods (Fig. 21), or by the transfer medium: refrigerants or coolant (e.g. water, glycol, oil, or acetone) (Fig. 22). Pesaran [159] and Bandhauer [10] qualitatively compared air and liquid method in terms of heat transfer coefficient, thermal conductivity, viscosity, density, and velocity of the fluid. The degree of temperature mal-distribution for the air-flow system due to lower specific heat and thermal conductivity seems to be significant. Using oil achieved the heat transfer coefficient 1.5 to 3 times higher than air [159]; and water or water/glycol, more than 3 times [10]. This indicates that the temperature difference will be reduced to 1/3 of that obtained from air, hence achieving fine temperature uniformity. Notably, the difference between using refrigerant and coolant is that the former does not require extra loops for chiller and heating elements. This implies that for battery preheating during winter, refrigerant will not be able to transfer heat energy to the battery thus can be less attractive. There are mainly three ways to achieve liquid BTM [159]: 1) through discrete tubing or a jacket around each battery module; 2) submerging modules in direct contact with a dielectric fluid (e.g. silicon-based or mineral oils) to avoid electrical shorts; and 3) positioning the modules onto liquid heated/cooled plates. The plates refer to thin metals having one or more internal channels discharged with refrigerant or coolant. Available external battery heating source during winter can be provided by using jacket or fluid heating from an electric heater [167, 168], a bioethanol heater (14.5 litres) used by Volvo C30 Electric [169], or a biogas (methane) engine proposed by Shimada [170].

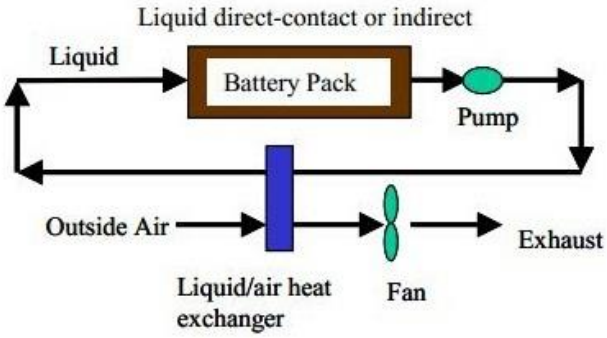

(a) Passive liquid cooling

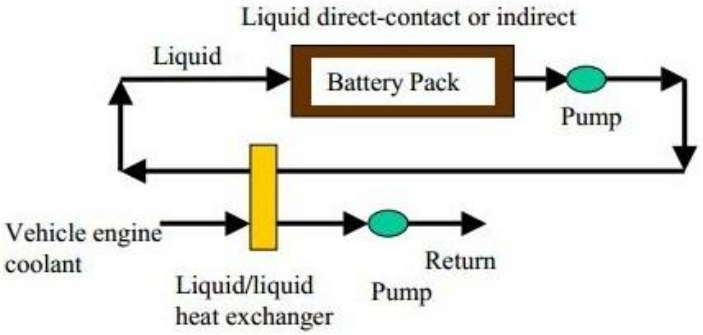

(b) Active moderate liquid cooling/heating

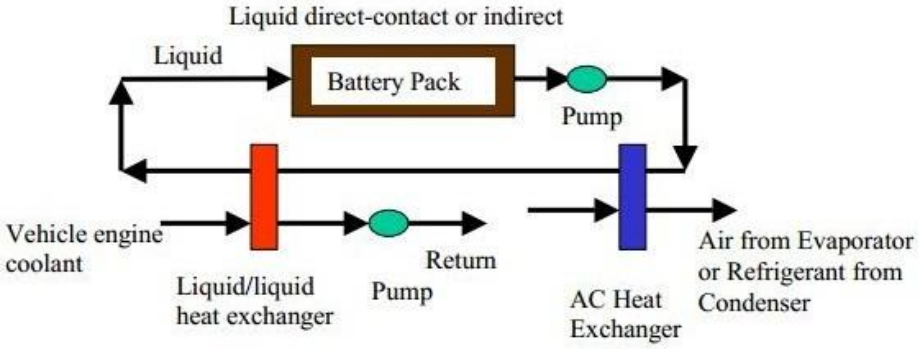

(c) Active liquid cooling/heating

Figure 21: Liquid BTM methods [159].

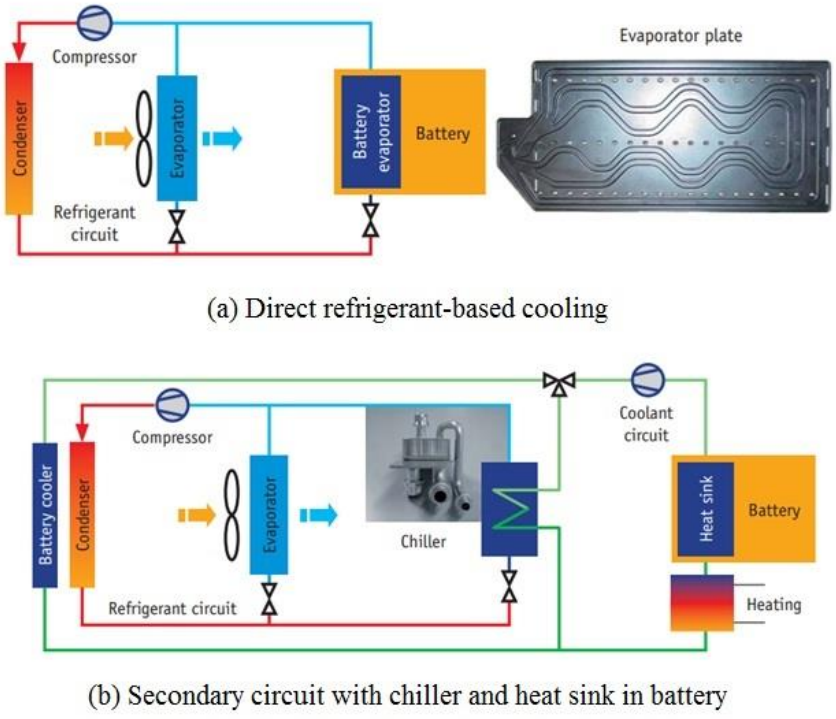

Figure 22: Liquid BTM using (a) refrigerant for battery cooling or (b) coolant for battery cooling/heating [163].

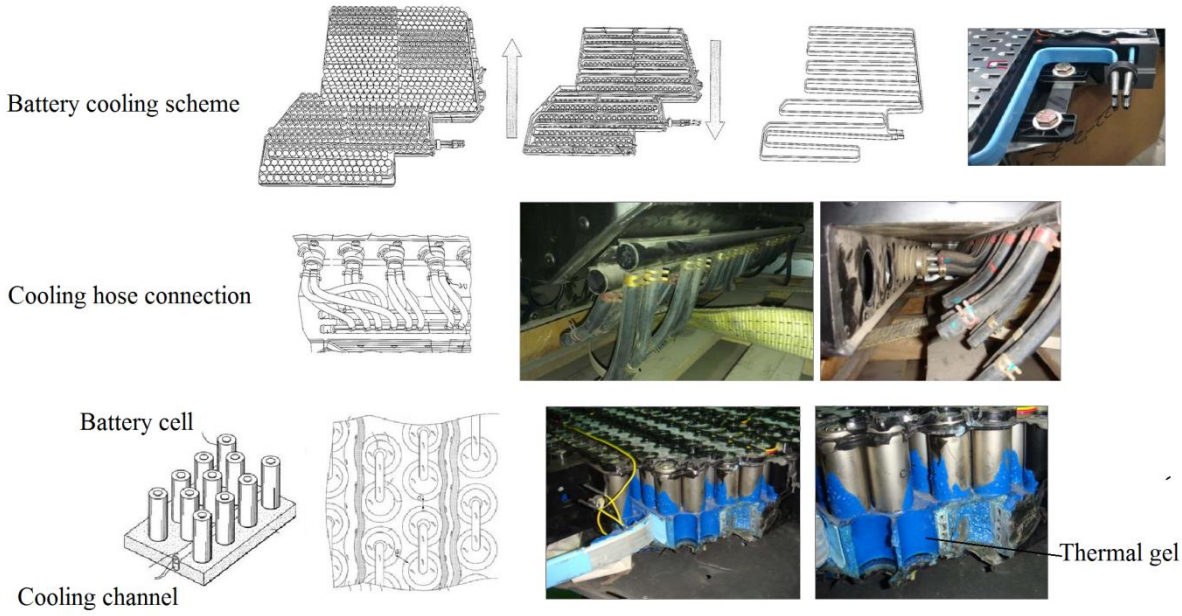

Figure 23: Tesla Roadster battery cooling (modified from [28, 62, 171, 172]).

Examples of liquid BTM used in cars can be found in [157, 159] with regard to different EV or HEV types; in [165] who investigated coolant cooling/heating for a Gen-2 lithium-ion batteries-based PNGV; in [163] that illustrates a direct refrigerant-based cooling in Mercedes S400 BlueHYBRID; and in [173] who reported active liquid cooling/heating implemented in Volt and Tesla. The battery

cooling system in Tesla Roadster uses water-glycol (1:1) mixture as coolant. A thermal interface (blue) is overmoulded onto the cooling tube forming a base below the battery pack (Fig. 23). This serves as a heat sink as the cooling liquid can be discharged in to provide efficient cooling. Improvements are suggested by Jarrett and Kim [174], who modelled serpentine-channel cooling plates in various geometries and concluded that 'a narrow inlet channel widening towards the outlet' is able to equalise the heat transfer achieving uniform temperature. Similarly, Faass and Clough [175] modified the cooling channel pathing geometry which produced an area of high turbulence and an area of low pressure drop. Jin et al. [176] proposed a novel minichannel liquid cold plate with oblique fins at optimised angle and width to cool EV batteries.

Table 12 lists strengths and weaknesses offered by air, refrigerant, and coolant BTM. Air BTM is suitable for all type of cells, whereas liquid BTM that usually adopts cooling/heating plates within the assembled battery cells prefers prismatic or pouch cell geometry. To summarise, air cooling takes up more space, adds up more weight due to additional air ducts and blowers, consumes larger compressor, generates potential noise disturbance, and is less effective at maintaining a uniform temperature. If the battery demands a tighter temperature control especially in some hotter environments, air is not as competitive as liquid. However, for refrigerant-based cooling, the battery cannot be heated in winter. Indeed, similar to batter cooling, battery heating seems to be also very important cooling because the performance of a cold battery is sluggish and may directly affect vehicle mobility and driving range. Therefore, using coolant is much preferred in liquid BTM. The trade-offs, however, are requirement of large space, extra weight, and increased complexity due to additional pumps, valves, chiller, and radiators. The ultimate concern is to either invest in an expensive but relatively compact liquid coolant system with higher battery power output, or a cheap but bulky air cooling system with low performance of the same battery size. No surprising, many automobile manufacturers would rather go for a cheaper option, which is to construct a slightly larger battery pack with air cooling system.

Table 12: A comparison among air, refrigerant and coolant BTM

	Advantages	**Disadvantages**
Air cooling/heating	• Suitable for all cell types • Simple • Cheap • Battery heating in winter	• Low heat transfer rate • Ineffective temperature uniformity • High space requirements • Additional weight problems • Potential noise disturbance
Refrigerant cooling	• High heat transfer rate • Allow battery to handle a larger pulse of power • Effective temperature uniformity • Low space requirements	• No battery warming • Electric shortage due to liquid leakage
Coolant cooling/heating	• High heat transfer rate • Allow battery to handle a larger pulse of power • Effective temperature uniformity	• Expensive (the most costly) • Electric shortage due to liquid leakage • High space requirements

	• Battery heating in winter	• Increased complexity and weight

4.2.3. PCM

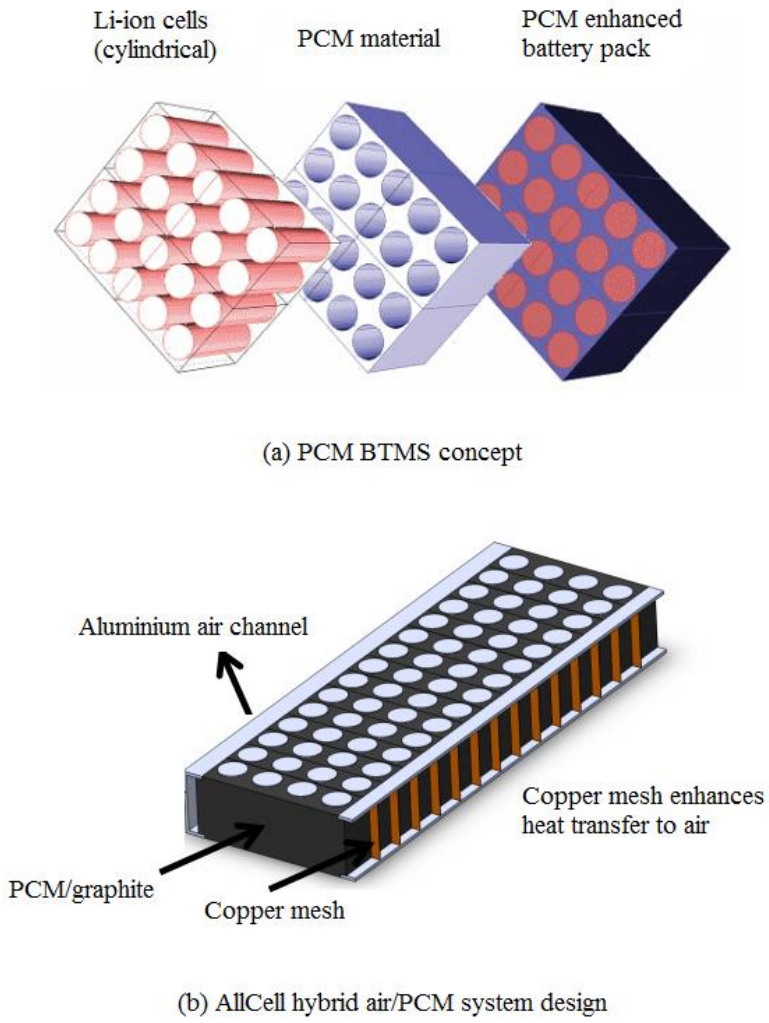

Figure 24: (a) PCM BTM concept; (b) AllCell hybrid air/PCM system design [177].

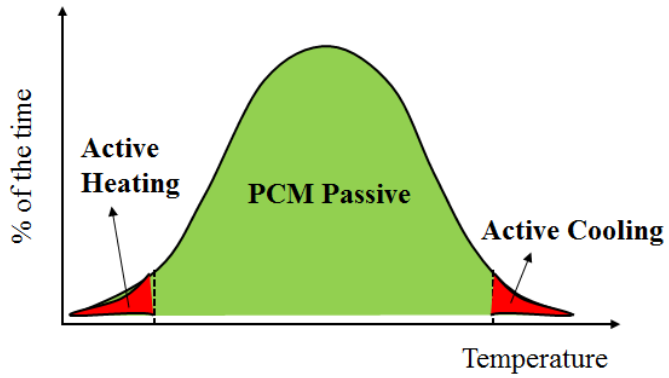

Figure 25: Hybrid air/PCM BTMS for EV normal operation

As an alternative method of direct liquid or air cooling/heating, researchers at Illinois Institute of Technology [140, 143, 178-181] pioneered a new passive BTM solution by using phase change material (PCM) (Fig. 24). A PCM normally has a large latent heat of fusion and a desirable melting point that can store or release large amounts of heat. The heat transfer route starts from the battery, which generates heat, and goes to the PCM and then to the battery case in contact with the ambient air. PCM eliminates the need for active cooling/heating during the majority of operating time because it delays the temperature rise when the ambient is cold and maintains the battery below ambient during hot days (Fig. 25). The battery module used in Fig. 24 was the commercial cylindrical 18650-lithium-ion-cells surrounded in a rectangular enclosure. The PCM is a paraffin wax with a melting temperature range from 40°C to 44°C and a latent heat of melting/solidification of 195 kJ/kg. The wax fills the voids in between the cells with solid and liquid phase densities of 822 and 910 kg/m^3, respectively. This reflects the lightweight advantage and material flexibility of the PCM. Rao et al. [182] listed the major criteria in selecting proper PCMs for BTM, and melting point comes to the first. This value should, as a matter of fact, be chosen in the range of the operating temperature that a battery desires. They stated that it is preferable to have a PCM with melting temperature below 45°C and a desired maximum temperature below 50°C to achieve effective heat dissipation and improved temperature uniformity across the whole battery unit.

In the study of Khateeb et al. [180], data showed that using PCM (paraffin wax), the centre cells temperature rised by 26.25-30°C while the edge cells rose only by 18.75-22.5°C. This indicates the poor thermal conductivity of PCM, and hence, it did not melt uniformly. The PCM near the centre cells was completely melted during the first discharge cycle, but those that near the cooled walls did not start melting until the third discharge cycle. If the PCM completely melts, an additional thermal resistance between the cooling fluid and the batteries will be created, leading to a worse situation than direct air cooling. Low thermal conductivity also becomes problematic when it comes to battery preheating in cold environments, and the thermal gradient among the cells can be huge if externally warmed. More importantly, the volume expansion after melting is inevitable, so additional volume spacing between the battery cells is required and leak-proof design to avoid PCM liquid leakage is crucial.

To reduce the thermal gradient inside the battery pack and solve the conflict between large heat storage capacity and low thermal conductivity (0.25 W/mK for paraffin wax), many approaches towards making composite PCMs have been conducted and they include 1) embedding a metal matrix into PCM; 2) impregnating porous materials [183-187]; 3) adding high thermal conductivity substances in paraffin [188, 189]; and 4) developing latent heat thermal energy storage systems with unfinned and finned structures [190-192]. The improved thermal conductivity for the composite PCM (PCM/graphite matrix) from references [140, 180, 181] ranges from 3 W/mK to 16.6 W/mK. Examples of using composite PCM in vehicular applications have been summarised in Table 13. However, the thermal conductivity increases at the cost of decreased latent heat storage capacity. In order to achieve a good performance, a proper thermal conductivity ratio between PCM and battery cells (k_{pcm}:k_c) must be ensured [182]. Moreover, with aim of eliminating battery safety risks, PCM properties such as stability, non-poisonous, non-flammable and non-explosive are critical. That is, a stable and stronger PCM based battery module to resist thermo-mechanical effects during operation is required. Alrashdan et al. [193] undertook a systematic experiment analysing the effects of the thermo-mechanical behaviours of paraffin wax/expanded graphite composite PCM for lithium-ion batteries. They observed that the increased percentage of paraffin wax will enhance tensile, compressive and burst strengths at room temperatures, but not so obvious under elevated temperatures.

Table 13: Composite PCMs in vehicular applications

Applications	Ref(s)	Composite PCM properties
For a large lithium-ion battery pack targeting at HEV/EV applications	Khateeb et al. [140] (electric scooters)	**PCM/aluminium foam:** $k_{eff} = k_{pcm}\varepsilon+(1-\varepsilon)k_{al}$, $\rho_{eff} = \rho_{pcm}\varepsilon+(1-\varepsilon)\rho_{al}$, $c_p = c_p\varepsilon+(1-\varepsilon)c_{p,al}$, h = 195 kJ/kg
	Sabbah [181]	**PCM/graphite matrix:** k_{eff} = 16.6 W/mK, ρ_{eff} = 866 kg/m^3, c_p = 1,980 J/kgK, T_m = 52-55ºC, h_{eff} = 181 kJ/kg
	AllCell Technologies LLC (AllCell®) [194]	**PCM/graphite matrix module**
	Kizilel et al. [143]	**PCM/graphite matrix:** k_{eff} = 16.6 W/mK, ρ_{eff} = 789 kg/m^3, c_p = 1,980 J/kgK, T_m = 42-45ºC, h_{eff} = 123 kJ/kg
	Li et al. [195]	**PCM/copper metal foam:** k_{eff} = 11.33/6.35/0.8 W/mK from different samples
For a comparison study based on a simulated single cylindrical battery cell	Duan [196]	**PCM 1** provided by the Glacier Tek Inc.: k_{pcm} = 0.55 W/mK, ρ_{pcm} = 840 kg/m^3, c_p = 2,100 J/kgK, T_m = 18ºC, h_{pcm} = 195 kJ/kg; **PCM 2** by Laird Technologies: k_{pcm} = 2.23 W/mK, c_p = 1,390 J/kgK, T_m = 50ºC
For cylindrical NiMH and rectangular lithium-ion batteries	Rao [182, 197, 198]	**PCM/graphite matrix:** parameters collected from references – not specified, ρ_{pcm} = 910 kg/m^3, T_m = 50ºC

4.2.4. Heat Pipe

Heat pipes are considered versatile in many industrial applications for their efficient cooling and thermal management [199], but heat pipe BTM has not been fully acknowledged [200-202]. Similar to the passive strategy offered by PCM, applying heat pipes to cool or heat the battery provides efficient heat transfer when and where needed at low power consumption. The mechanism of a heat pipe is that the heat can be transferred through latent heat of vaporisation from the evaporator to the condenser, and the working fluid can be passively transport back to the evaporator by capillary pressure developed within a porous wick lining. Operating in this fashion, the heat can be continuously absorbed and released.

The combination of heat pipe and air cooling was adopted in early studies. For instance, Swanepoel [203] proposed to use pulsating heat pipes (PHPs) to thermally manage Optima Spirocell lead acid batteries and control HEV components. Simulation and experiment results showed that a well-designed PHP system required the diameter of the heat pipe to be less than 2.5mm and ammonia as working fluid. Wu et al. [204] suggested to use the heat pipes with aluminium fins to cool a large-scale lithium-ion battery but difficulties in heat dissipation at the battery centre were found if no cooling fan at the condenser section was provided. Jang and Rhi [205] used a loop thermosyphon cooling method which also combined the heat pipe with air cooling. Barantsevich and Shabalkin [206] introduced the testing aspects of ammonia axial grooved heat pipes to thermally control the solar battery drive, and Park et al. [207] obtained a numerical optimisation for a loop heat pipe to cool the lithium-ion battery onboard a military aircraft. More recently, Burban et al. [208] tested an unlooped PHP (2.5mm inner tube diameter) with an air heat exchanger for cooling electronic devices in hybrid vehicles (Fig. 26). Steady state and transient performance with a hybrid driving cycle (New European Driving Cycle) were conducted and various heat pipe working fluids, inclinations, and different air speeds were investigated. Moreover, Tran et al. [209] proposed a flat heat pipe for cooling HEV lithium-ion batteries under natural and forced convection and highlighted the thermal performance under various heat pipe positions (Fig. 27).

The combination of heat pipe and liquid cooling is scarce and the example can only be found in Rao et al. [210], who experimentally examined the heat pipe based battery cooling for commercial prismatic $LiFePO_4$ batteries. The condenser of the heat pipe was cooled by a water bath at 25±0.05°C (Fig. 28). It seems that the heat pipe has the potential of handling increased heat flux more efficiently than the conventional heat sink, but the feasibility of applying heat pipes into vehicle batteries needs to be further examined. Factors such as cost, weight, mass production, material compatibility, transient behaviour under high frequency and large amplitude variable input power, and thermal performance degradation influenced by vehicle shock and vibration should be evaluated. Unlike air and liquid BTM, heat pipe BTM is still under initial development. It is therefore encouraged that the research may be extended at pack level such that the impact of thermal accumulation from various cycle performances could be fully understood.

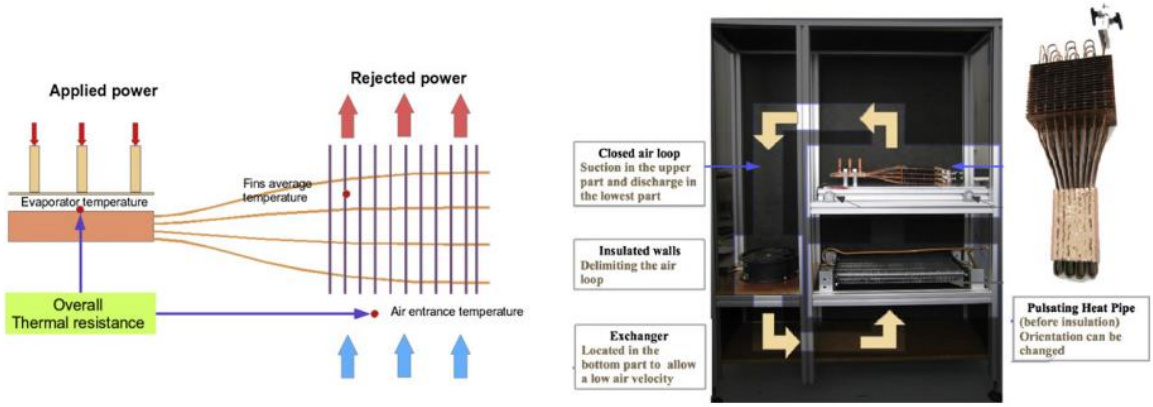

Figure 26: Pulsating heat pipe cooling a HEV lithium-ion battery pack [208].

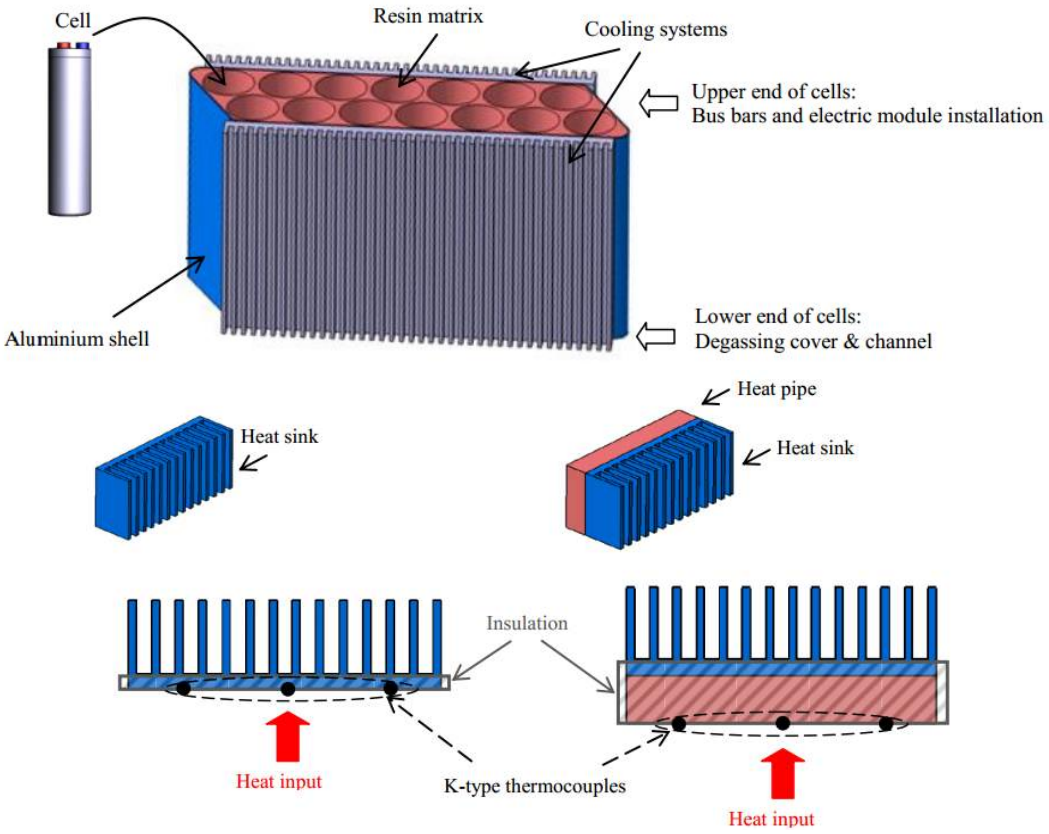

Figure 27: Flat heat pipe cooling a HEV lithium-ion battery pack [209].

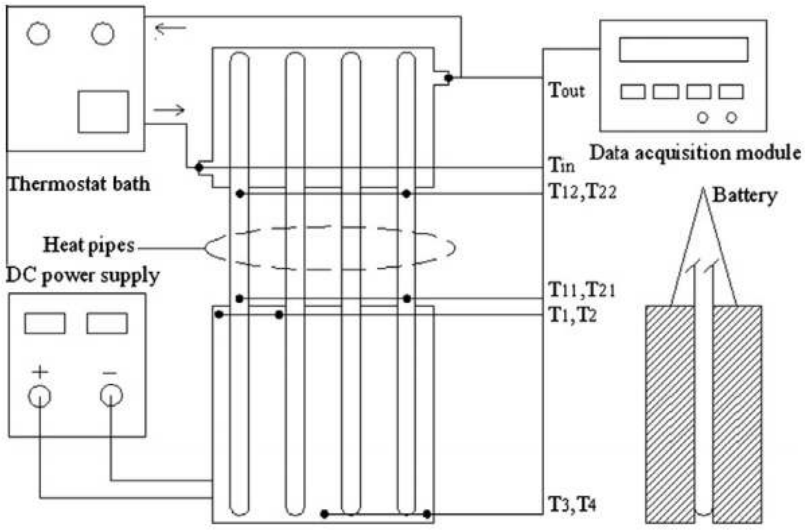

Figure 28: Cylindrical flattened heat pipe cooling for a 118*63*13mm 8Ah LiFePO4 battery pack [210].

5. Conclusions

This paper reviews the thermal models and thermal management solution of lithium-ion batteries used for HEVs and EVs. The battery thermal model can be either thermal-electrochemical coupled or decoupled, depending on the heat generation. The fully coupled model uses newly generated parameters from electrochemical model to calculate the heat generation, while the decoupled model employs empirical equations based on experimental data.

Many experimental measurements have been conducted based on small cells at low charge/discharge rate near ambient temperatures, thus a standalone thermal model for the entire battery pack may not be sufficient accurate for predicting the thermal behaviour.

BTM has played an essential role in eliminating thermal impacts of lithium-ion batteries, which improves temperature uniformity across the batter pack, prolongs battery lifespan, and enhances the safety of large packs. Temperature effects, heat sources and sinks, EV/HEV batteries, and temperature control should be considered before designing a good battery thermal management The thermal management strategies can be either internal or external. Limited internal BTM for lithium-ion batteries was reported which needs further investigation. BTM external to the batteries has been discussed extensively and they are categorised based on medium: air, liquid, PCM, heat pipe, or the combinations. Cheap air BTM is suitable for all cell configurations but the majority use is for NiMH battery packs in HEVs. Liquid BTM is regarded as a better solution compared to air and has been commercialised in cooling lithium-ion batteries in Mercedes S400 BlueHYBRID and Tesla Roadster.

In addition, PCM comes to consideration for that it eliminates the need for active cooling/heating during the majority of operating time, but low thermal conductivity becomes problematic when it comes to battery cooling or preheating. Using heat pipes for BTM is relatively new and the potential of combing heat pipes with air or liquid cooling needs to be further explored. Finding the cheapest, lightest and the most effective solution such as PCM and heat pipe is important to provide efficient heat transfer at low power consumption, but research should be extended at pack level such that the impact of thermal accumulation from various cycle performances could be fully understood.

Acknowledgement:

This project is partially supported by the R&D Centre, FAW Group.

References

[1] S. Amjad, S. Neelakrishnan, and R. Rudramoorthy, "Review of design considerations and technological challenges for successful development and deployment of plug-in hybrid electric vehicles," *Renewable and Sustainable Energy Reviews,* vol. 14, pp. 1104-1110, 2010.

[2] V. Oikonomou, F. Becchis, L. Steg, and D. Russolillo, "Energy saving and energy efficiency concepts for policy making," *Energy Policy,* vol. 37, pp. 4787-4796, 2009.

[3] M. Wada, " Research and development of electric vehicles for clean transportation," *Journal of Environmental Sciences-China,* vol. 21, pp. 745-749, 2009.

[4] G. G. Harding, "Electric vehicles in the next millennium," *Journal of Power Sources,* vol. 78, pp. 193-198, 1999.

[5] K. T. Chau and Y. S. Wong, "Hybridization of energy sources in electric vehicles," *Energy Conversion and Management,* vol. 42, pp. 1059-1069, 2001.

[6] S. Eaves and J. Eaves, "A cost comparison of fuel-cell and battery electric vehicles," *Journal of Power Sources,* vol. 130, pp. 208-212, 2004.

[7] P. H. Andersen, J. A. Mathews, and M. Rask, "Integrating private transport into renewable energy policy: the strategy of creating intelligent recharging grids for electric vehicles," *Energy Policy,* vol. 37, pp. 2481-2486, 2009.

[8] E. Endo, "Market penetration analysis of fuel cell vehicles in Japan by using the energy system model MARKAL," *International Journal of Hydrogen Energy,* vol. 32, pp. 1347-1354, 2007.

[9] S. Brown, D. Pyke, and P. Steenhof, "Electric vehicles: the role and importance of standards in an emerging market," *Energy Policy,* vol. 38, pp. 3797-3806, 2010.

[10] T. M. Bandhauer, S. Garimella, and T. F. Fuller, "A Critical Review of Thermal Issues in Lithium-ion Batteries," *Journal of Electrochemical Society,* vol. 158, pp. R1-R25, 2011.

[11] K. T. Chau, Y. S. Wong, and C. C. Chan, "An overview of energy sources for electric vehicles," *Energy Conversion and Management,* vol. 40, pp. 1021-1039, 1999.

[12] Y. Hirota and S. Ogasawara, *Electric Vehicle Engineering*. Morikita, Tokyo, 2010.

[13] M. Shimada, "Magnetic Materials in Vehicles Driven by Electricity," presented at the The 2010 Hirosaki University International Symposium, The 2nd International Symposium: Energy and Environment in Aomori, Hirosaki, 2011.

[14] DieselNet. (2012). *Emission Test Cycles: Japanese 10-15 Mode*. Available: http://www.dieselnet.com/standards/cycles/jp_10-15mode.php

[15] E. D. Wachsman and K. T. Lee, "Lowering the Temperature of Solid Oxide Fuel Cells," *Science,* vol. 334, pp. 935-939, 2011.

[16] D. Linden, *Handbook of Batteries*, 3rd ed. New York: McGraw-Hill, 2002.

[17] J. Axsen, A. Burke, and K. Kurani, "Batteries for Plug-in Hybrid Electric Vehicles (PHEVs): Goals and the State of Technology circa 2008," Institute of Transportation Studies, Davis, CA2008.

[18] C. Cluzel and C. Douglas, "Cost and Performance of EV Batteries," Element Energy Limited2012.

[19] L. Gaines and R. Cuenca, "Costs of Lithium-Ion Batteries for Vehicles," Argonne National Laboratory2000.

[20] E. Hsiao and C. Richter, "Electric Vehicles: Special Report," CLSA2008.
[21] C. E. Irwin, "Energy Storage: CleanTech Industry Report," Merriman Curhan Ford2008.
[22] R. Lache, P. Nolan, D. Galves, G. Toulemonde, J. Gehrke, K. Sanger, V. Ha, S. Rao, and J. Crane, "Electric Cars: Plugged In - Batteries must be included," Deutsche Bank Securities Inc.2008.
[23] V. Srinivasan, "Batteries for Vehicular Applications," Lawrence Berkeley National Lab, Berkeley, CA2008.
[24] M. H. Westbrook, *The Electric Car: Development and Future of Battery, Hybrid and Fuel-cell Cars*. London: The Institution of Electrical Engineers, 2001.
[25] Daimler. Daimler analysis [Online]. Available: http://www.daimler.com/
[26] RECHARGE, "Safety of lithium-ion batteries," The European Association for Advanced Rechargeable Batteries2013.
[27] A123Systems. (2008). *Pulg-in: PHEV Safety*. Available: http://www.a123systems.com/applications/plug-in-hybrid
[28] Doug. (2010). *Roadster battery (ESS)*. Available: http://www.teslamotorsclub.com/showthread.php/3810-Roadster-battery-(ESS)
[29] TeslaMotor. *Increasing energy density means increasing range*. Available: http://www.teslamotors.com/sv_SE/roadster/technology/battery
[30] *Leaf's Battery Pack*. Available: http://www.teslamotorsclub.com/attachment.php?attachmentid=2534
[31] Wikipedia. (2014). *BMW i3*. Available: http://en.wikipedia.org/wiki/BMW_i3
[32] Wikipedia. (2014). *BYD e6*. Available: http://en.wikipedia.org/wiki/BYD_e6
[33] Wikipedia. (2014). *Chevrolet Spark*. Available: http://en.wikipedia.org/wiki/Chevrolet_Spark_EV
[34] J. van Agt. Electric Car Citroën C-Zero [Online]. Available: http://www.olino.org/us/articles/2010/07/22/electric-car-citroen-c-zero
[35] Wikipedia. (2014). *Mitsubishi i-MiEV*. Available: http://en.wikipedia.org/wiki/Mitsubishi_i-MiEV
[36] Wikipedia. (2014). *Ford Focus Electric*. Available: http://en.wikipedia.org/wiki/Ford_Focus_Electric
[37] Wikipedia. (2014). *Nissan Leaf*. Available: http://en.wikipedia.org/wiki/Nissan_Leaf
[38] Wikipedia. (2014). *Tesla Model S*. Available: http://en.wikipedia.org/wiki/Tesla_Model_S
[39] Wikipedia. (2014). *Venturi Fétish*. Available: http://en.wikipedia.org/wiki/Venturi_F%C3%A9tish
[40] Wikipedia. (2014). *Volkswagen Up*. Available: http://en.wikipedia.org/wiki/Volkswagen_Up
[41] P. Scott and M. Burton. The New BMW i3 [Online]. Available: http://www.asymcar.com/graphics/14/i3/bmwi3b.pdf
[42] J. Cole. First BMW i3 Electric Car Test Ride, 2.3 Gallon Range Extender Option To Cost About $4,000 [Online]. Available: http://insideevs.com/first-bmw-i3-electric-car-test-ride-2-3-gallon-range-extender-option-to-cost-about-4000/
[43] (2010). *BYD: Only 1,000 E6s for 2010*. Available: http://chinaautoweb.com/2010/06/byd-only-1000-e6s-for-2010/
[44] T. Woody, "From China to Los Angeles, Taking the Electric Bus," in *The New York Times*, ed, 2013.

[45] M. Wayland, "GM insourcing Chevy Spark EV battery production," in *mlive*, ed, 2014.
[46] Chevrolet. [Online]. Available: http://www.chevrolet.com/
[47] D. Glynne Jones. Mitsubishi i-MiEV drive [Online]. Available: https://www.sia.org.au/downloads/Divisional/ACT/i-MiEV_presentation.pdf
[48] S. Bähnisch, "Im Prinzip gut," in *Autobild*, ed, 2010.
[49] Greencarcongress. (2010). *Mitsubishi Motors to Premiere the European-spec i-MiEV at the 2010 Paris Motor Show*. Available: http://www.greencarcongress.com/2010/08/mitsubishi-motors-to-premiere-the-european-spec-i-miev-at-the-2010-paris-motor-show.html#more
[50] A. Charlton, "Ford Focus Electric: First Drive," in *International Business Times*, ed, 2013.
[51] Ford. (2014). *Ford Focus Electric*. Available: http://www.ford.com/cars/focus/trim/electric/
[52] I. N. Laboratory. 2011 Nissan Leaf – VIN 0356 Advanced Vehicle Testing – Beginning-of-Test Battery Testing Results [Online]. Available: http://media3.ev-tv.me/DOEleaftest.pdf
[53] TeslaMotorForum. (2011). *The Model S Battery*. Available: http://www.teslamotors.com/fr_CA/forum/forums/model-s-battery-0
[54] TeslaMotor. (2014). Available: http://www.teslamotors.com/
[55] VenturiFetish. (2014). *Venturi Fetish, top of the art of technology*. Available: http://www.ventec-bms.com/venturi-fetish/
[56] J. Lard. (2014). *Volkswagen's new e-up! electric car is shockingly good*. Available: http://www.techradar.com/news/car-tech/volkswagen-s-e-up-electric-car-is-shockingly-good-1223000
[57] Wikipedia. (2010). *List of production battery electric vehicles (table)*. Available: http://en.wikipedia.org/wiki/List_of_production_battery_electric_vehicles_(table)
[58] T. Cunningham. (2010). *Th!nk City*. Available: http://www.oeva.org/presentations/THINKPresentationMar11_2010.pdf
[59] Wikipedia. (2014). *General Motors*. Available: http://en.wikipedia.org/wiki/General_Motors_EV1#Battery
[60] USDOE. (1999). *1999 General Motors EV1 w/NiMH - vehicle specifications*. Available: http://avt.inel.gov/pdf/fsev/eva/ev1_eva.pdf
[61] C. Madrid, J. Argueta, and J. Smith. (1999). *Performance Characterization*. Available: http://avt.inel.gov/pdf/fsev/sce_rpt/altra_report.pdf
[62] G. Berdichevsky, K. Kelty, J. B. Straubel, and E. Toomre, "The Tesla Roadster Battery System," 2006.
[63] D. Doughty and E. P. Roth, "A general discussion of Li-ion battery safety," *The Electrochemical Society Interface,* vol. 21, pp. 37-44, 2012.
[64] ISO, "ISO 6469-1:2009: Electrically propelled road vehicles - Safety specifications," ed, 2009.
[65] S. C. Levy and P. Bro, *Battery hazards and accident prevention* New York: Plenum Press, 1994.
[66] E. P. Roth, C. C. Crafts, D. H. Doughty, and J. McBreen, "Advanced Technology Development Program for Lithium-Ion Batteries: Thermal Abuse Performance of 18650 Li-Ion Cells," Sandia National Laboratories2004.
[67] D. H. Doughty, "Li-ion battery abuse tolerance testing - an overview," Sandia National Laboratories2006.

[68] P. G. Balakrishnan, R. Ramesh, and T. P. Kumar, "Safety mechanisms in lithium-ion batteries," *Journal of Power Sources,* vol. 155, pp. 401-414, 2006.
[69] (2012). *Investigation concludes fire in BYD e6 collision caused by electric arcs from short circuit igniting interior materials and part of power battery*. Available: http://www.greencarcongress.com/2012/08/byde6-20120810.html
[70] J. Christopher, "Chevy Volt Fire Prompts Federal Investigation Into Lithium-Ion Batteries," in *The New York Times*, ed, 2011.
[71] J. Voelcker, "Chrysler Yanks Plug-In Hybrid Test Fleet Off Roads, Will Replace Batteries," in *Green Car Report*, ed, 2012.
[72] F. Automotive, "Fisker: Karma fire caused by fault in low-temperature cooling fan; initiates recall," in *Green Car Congress*, ed, 2012.
[73] E. Loveday, "Mitsubishi Extends Production Halt on Outlander PHEV as Perplexing Battery Investigation Continues," in *InsideEVs*, ed, 2013.
[74] E. Musk. (2013). *Model S Fire*. Available: http://www.teslamotors.com/blog/model-s-fire
[75] (2011). *Battery Pack Defects Blamed for Zotye EV Fire*. Available: http://chinaautoweb.com/2011/06/battery-pack-defects-blamed-for-zotye-ev-fire/
[76] H. P. Lin, D. Chua, M. Salomon, H. C. Shiao, M. Hendrickson, E. Plichta, and S. Slane, "Low-temperature behavior of Li-ion cells," *Electrochemical and Solid-State Letters* vol. 4, pp. A71-A73, 2001.
[77] NissanUSA. (2012). *How conditions affect range*. Available: http://www.nissanusa.com/leaf-electric-car/range?next=ev_micro.section_nav
[78] U. S. A. B. C. (USABC), "Electric vehicle battery test procedures manual," ed, 1996.
[79] *QC/T 743-2006: Lithium-ion Batteries for Electric Vehicles*, 2006.
[80] C. K. Huang, J. S. Sakamoto, J. Wolfenstine, and S. Surampudi, "The limits of low-temperature performance of Li-ion cells," *Journal of Electrochemical Society,* vol. 147, pp. 2893-2896, 2000.
[81] G. Nagasubramanian, "Electrical characteristics of 18650 Li-ion cells at low temperatures," *Journal of Applied Electrochemistry,* vol. 31, pp. 99-104, 2001.
[82] N. Shidore and T. Bohn, "Evaluation of cold temperature performance of the JCS-VL41M PHEV battery using Battery HIL," 2008.
[83] J. Fan and S. Tan, "Studies on charging lithium-ion cells at low temperatures," *Journal of Electrochemical Society,* vol. 153, pp. A1081-A1092, 2006.
[84] S. S. Zhang, K. Xu, and T. R. Jow, "The low temperature performance of Li-ion batteries," *Journal of Power Sources,* vol. 115, pp. 137-140, 2003.
[85] R. X. Shi, Q. Xia, J. Yang, and Z. Ling, "Low Temperature Performance Analysis of Li-ion Batteries for Electric Vehicles," *Bus & Coach Technology and Research,* p. 3, 2012.
[86] S. S. Zhang, K. Xu, and T. R. Jow, "Electrochemical impedance study on the low temperature of Li-ion batteries," *Electrochimica Acta,* vol. 49, pp. 1057-1061, 2004.
[87] Y. Ji and C. Y. Wang, "Heating strategies for Li-ion batteries operated from subzero temperatures," *Electrochimica Acta,* vol. 107, pp. 664-674, 2013.
[88] M. C. Smart, B. V. Ratnakumar, and S. Surampudi, "Electrolytes for low-temperature lithium batteries based on ternary mixtures of aliphatic carbonates," *Journal of Electrochemical Society,* vol. 146, pp. 486-492, 1999.

[89] E. J. Plichta and W. K. Behl, "A low-temperature electrolyte for lithium and lithium-ion batteries," *Journal of Power Sources,* vol. 88, pp. 192-196, 2000.
[90] C. S. Wang, J. A. Appleby, and F. E. Little, "Low-temperature characterization of lithium-ion carbon anodes via microperturbation measurement," *Journal of Electrochemical Society,* vol. 2002, pp. A754-A760, 2002.
[91] S. S. Zhang, K. Xu, and T. R. Jow, "Charge and discharge characteristics of a commercial LiCoO2-based 18650 Li-ion battery," *Journal of Power Sources,* vol. 160, pp. 1403-1409, 2006.
[92] T. A. Stuart and A. Hande, "HEV battery heating using AC currents," *Journal of Power Sources,* vol. 129, pp. 368-378, 2004.
[93] S. S. Zhang, K. Xu, and T. R. Jow, "Study of LiBF4 as an electrolyte salt for a Li-ion battery," *Journal of Electrochemical Society,* vol. 149, pp. A586-A590, 2002.
[94] J. L. Allen, T. R. Jow, and J. Wolfenstine, "LiCoPO4 as Li-ion cathode," *ECS Transactions,* vol. 41, pp. 15-20, 2012.
[95] G. G. Botte, V. R. Subramanian, and R. E. White, "Mathematical Modeling of Secondary Lithium Batteries," *Electrochimica Acta,* vol. 45, pp. 2595-2609, 2000.
[96] W. B. Gu and C. Y. Wang, "Thermal-electrochemical modeling of battery systems," *Journal of the Electrochemical Society,* vol. 147, pp. 2910-2922, 2000.
[97] C. R. Pals and J. Newman, "Thermal Modeling of the Lithium/Polymer Battery: II. Temperature Profiles in a Cell Stack," *Journal of Electrochemical Society,* vol. 142, pp. 3282-3288, 1995.
[98] M. Doyle, T. F. Fuller, and J. Newman, "Modeling of Galvanostatic Charge and Discharge of the Lithium/Polymer/Insertion Cell " *Journal of Electrochemical Society,* vol. 140, pp. 1526-1533, 1993.
[99] T. F. Fuller, M. Doyle, and J. Newman, "Simulation and Optimization of the Dual Lithium Ion Insertion Cell," *Journal of Electrochemical Society,* vol. 141, pp. 1-10, 1994.
[100] J. Newman, *Electrochemical Systems*: Prentice Hall, 1991.
[101] M. Doyle and J. Newman, "Comparison of Modeling Predictions with Experimental Data from Plastic Lithium Ion Cells," *Journal of Electrochemical Society,* vol. 143, pp. 1890-1903, 1996.
[102] H. W. He, R. Xiong, and J. X. Fan, "Evaluation of Lithium-ion Battery Equivalent Circuit Models for State of Charge Estimation by an Experimental Approach " *Energies,* vol. 4, pp. 582-598, 2011.
[103] V. H. Johnson, A. A. Pesaran, and T. Sack, "Temperature-Dependent Battery Model for High-Power Lithium-Ion Batteries," presented at the 17th Electric Vehicle Symposium, Montreal, Canada, 2000.
[104] V. H. Johnson, "Battery performance models in ADVISOR," *Journal of Power Sources,* vol. 110, pp. 321-329, 2002.
[105] T. Markel, A. Brooker, T. Hendricks, V. Johnson, K. Kelly, B. Kramer, M. O'Keefe, S. Sprik, and K. Wipke, "ADVISOR: a system analysis tool for advanced vehicle modeling," *Journal of Power Sources,* vol. 110, pp. 255-266, 2002.
[106] S. Lee, J. Kim, J. Lee, and B. H. Cho, "State-of-charge and capacity estimation of lithium-ion battery using a new open-circuit voltage versus state-of-charge," *Journal of Power Sources,* vol. 185, pp. 1367-1373, 2008.

[107] T. Huria, M. Ceraolo, J. Gazzarri, and R. Jackey, "High Fidelity Electrical Model with Thermal Dependence for Characterization and Simulation of High Power Lithium Battery Cells," presented at the IEEE International Electric Vehicle Conference 2012.
[108] J. Feng, H. F. He, and G. F. Wang, "Comparison Study of Equivalent Circuit Model of Li-Ion Battery for Electrical Vehicles," *Research Journal of Applied Sciences,* vol. 6, pp. 3756-3759, 2013.
[109] G. H. Kim and K. Smith, "Three-Dimensional Lithium-Ion Battery Model," presented at the 4th International Symposium on Large Lithium Ion Battery Technology and Application Tampa, Florida, 2008.
[110] K. J. Lee, K. Smith, and G. H. Kim, "A Three-Dimensional Thermal-Electrochemical Coupled Model for Spirally Wound Large-Format Lithium-Ion Batteries," presented at the Space Power Workshop, Los Angeles, CA, 2011.
[111] X. F. Lin, H. E. Perez, S. Mohan, J. B. Siegel, A. G. Stefanopoulou, Y. Ding, and M. P. Castanier, "A lumped-parameter electro-thermal model for cylindrical batteries," *Journal of Power Sources,* vol. 257, pp. 1-11, 2014.
[112] T. M. Bandhauer, S. Garimella, and T. F. Fuller, "Electrochemical-thermal modeling and microscale phase change for passive internal thermal management of lithium ion batteries," Sandia National Laboratories 2012.
[113] D. Bernardi, E. Pawlikowski, and J. Newman, "A general energy balance for battery systems," *Journal of Electrochemical Society,* vol. 132, pp. 5-12, 1985.
[114] J. S. Hong, H. Maleki, S. A. Hallaj, L. Redey, and J. R. Selman, "Electrochemical-Calorimetric Studies of Lithium-ion Cells," *Journal of the Electrochemical Society,* vol. 145, pp. 1489-1501, 1998.
[115] N. Sato, "Thermal Behaviour analysis of lithium-ion batteries for electric and hybrid vehicles," *Journal of Power Sources,* vol. 99, pp. 70-77, 2001.
[116] K. Smith and C. Y. Wang, "Power and thermal characterization of a lithium-ion battery pack for hybrid-electric vehicles," *Journal of Power Sources,* vol. 160, pp. 662-673, 2006.
[117] W. F. Fang, O. J. Kwon, and C. Y. Wang, "Electrochemical–thermal modeling of automotive Li-ion batteries and experimental validation using a three-electrode cell," *Journal of Energy Research,* vol. 34, pp. 107-115, 2010.
[118] E. Prada, D. D. Domenico, Y. Creff, J. Bernard, V. Sauvant-Moynot, and F. Huet, "Simplified Electrochemical and Thermal Model of LiFePO4-Graphite Li-Ion Batteries for Fast Charge Applications," *Journal of the Electrochemical Society,* vol. 159, pp. A1508-A1519, 2012.
[119] V. Srinivasan and C. Y. Wang, "Analysis of Electrochemical and Thermal Behavior of Li-Ion Cells," *Journal of The Electrochemical Society,* vol. 150, pp. A98-A106, 2003.
[120] L. Song and J. W. Evans, "Electrochemical-thermal model of lithium polymer batteries," *Journal of Electrochemical Society,* vol. 147, pp. 2086-2095, 2000.
[121] P. M. Gomadam, J. W. Weidner, R. A. Dougal, and R. E. White, "Mathematical modeling of lithium-ion and nickel battery systems," *Journal of Power Sources,* vol. 110, pp. 267-284, 2002.
[122] W. B. Gu and C. Y. Wang, "Thermal-electrochemical coupled modeling of a lithium-ion cell," *ECS Proceedings,* vol. 99, pp. 748-762, 2000.

[123] G. H. Kim and K. Smith, "Multi-dimensional electrochemical-thermal coupled model of large format cylindrical lithium ion cells," presented at the 212th ECS Meeting, Washington, DC, 2007.
[124] L. Cai and R. E. White, "Mathematical modeling of a lithium ion battery with thermal effects in COMSOL Inc. Multiphysics (MP) software," *Journal of Power Sources,* vol. 196, pp. 5985-5989, 2011.
[125] D. R. Baker and M. W. Verbrugge, "Temperature and Current Distribution in Thin-Film Batteries," *Journal of the Electrochemical Society,* vol. 146, pp. 2413-2424, 1999.
[126] P. Taheri and M. Bahrami, "Temperature Rise in Prismatic Polymer Lithium-ion Batteries: An Analytic Approach," *SAE International Journal of Passengers Cars - Electronic and Electrical Systems,* vol. 5, pp. 164-176, 2012.
[127] Y. Chen and J. W. Evans, "Heat transfer phenomena in lithium/polymer-electrolyte batteries for electric vehicle application," *Journal of the Electrochemical Society,* vol. 140, pp. 1833-1838, 1993.
[128] Y. F. Chen and J. W. Evans, "Three-dimensional thermal modeling of lithium-polymer batteries under galvanostatic discharge and dynamic power profile," *Journal of Electrochemical Society,* vol. 141, pp. 2947-2955, 1994.
[129] Y. F. Chen and J. W. Evans, "Thermal analysis of lithium-ion batteries," *Journal of Electrochemical Society,* vol. 143, pp. 2708-2712, 1996.
[130] S. Al-Hallaj, H. Maleki, J. S. Hong, and J. R. Selman, "Thermal modelling and design considerations of lithium-ion batteries," *Journal of Power Sources,* vol. 83, pp. 1-8, 1999.
[131] S. A. Hallaj, J. Prakash, and J. R. Selman, "Characterization of commercial Li-ion batteries using electrochemical-calorimetric measurements " *Journal of Power Sources,* vol. 87, pp. 186-194, 2000.
[132] S. C. Chen, C. C. Wan, and Y. Y. Wang, "Thermal Analysis of Lithium-ion Batteries," *Journal of Power Sources,* vol. 140, pp. 111-124, 2005.
[133] K. Onda, T. Ohshima, M. Nakayama, K. Fukuda, and T. Araki, "Thermal behavior of small lithium-ion battery during rapid charge and discharge cycles," *Journal of Power Sources,* vol. 158, pp. 535-542, 2006.
[134] S. C. Chen, Y. Y. Wang, and C. C. Wan, "Thermal Analysis of Spirally Wound Lithium Batteries," *Journal of Electrochemical Society,* vol. 153, pp. A637-A648, 2006.
[135] U. S. Kim, C. B. Shin, and C. S. Kim, "Effect of electrode configuration on the thermal behavior of a lithium-polymer battery," *Journal of Power Sources,* vol. 180, pp. 909-916, 2008.
[136] U. S. Kim, C. B. Shin, and C. S. Kim, "Modeling for the scale-up of a lithium-ion polymer battery," *Journal of Power Sources,* vol. 189, pp. 841-846, 2009.
[137] A. A. Pesaran, "Battery thermal models for hybrid vehicle simulations," *Journal of Power Sources,* vol. 110, pp. 337-382, 2002.
[138] A. A. Pesaran, M. Keyser, G. H. Kim, S. Santhanagopalan, and K. Smith, "Tools for Designing Thermal Management of Batteries in Electric Drive Vehicles," presented at the the Large Lithium Ion Battery Technology & Application Symposia Advanced Automotive Battery Conference Pasadena, CA, 2013.
[139] F. Ladrech, "Battery Thermal Management for HEV & EV – Technology overview," presented at the Automotive Summit, 2010.

[140] S. A. Khateeb, S. Amiruddin, M. Farid, J. R. Sleman, and S. Al-Hallaj, "Thermal management of Li-ion battery with phase change material for electric scooter: experiment validation," *Journal of Power Sources,* vol. 142, pp. 345-353, 2005.

[141] L. G. Lu, X. B. Han, J. Q. Li, J. F. Hua, and M. G. Ouyang, "A review on the key issues for lithium-ion battery management in electric vehicles," *Journal of power Sources,* vol. 226, pp. 272-288, 2013.

[142] Z. H. Rao and S. F. Wang, "A review of power battery thermal energy management," *Renewable and Sustainable Energy Reviews,* vol. 15, pp. 4554-4571, 2011.

[143] R. Kizilel, R. Sabbah, J. R. Selman, and S. Al-Hallaj, "An alternative cooling system to enhance the safety of Li-ion battery packs," *Journal of Power Sources,* vol. 194, pp. 1105-1112, 2009.

[144] R. Mahamud and C. W. Park, "Reciprocating air flow for Li-ion battery thermal management to improve temperature uniformity," *Journal of Power Sources,* vol. 196, pp. 5685-5696, 2011.

[145] Panasonic. (2007). *Overview: Lithium Ion Batteries*. Available: http://industrial.panasonic.com/www-data/pdf/ACA4000/ACA4000PE3.pdf

[146] B. Lawson. *Battery and Energy Technologies*. Available: http://www.mpoweruk.com/thermal.htm

[147] W. Waag, S. Kabitz, and D. U. Sauer, "Experimental investigation of the lithium-ion battery impedance characteristic at various conditions and aging states and its influence on the application," *Applied Energy,* vol. 102, pp. 885-897, 2013.

[148] P. Ramadassm, B. Haran, R. White, and B. N. Popov, "Capacity fade of Sony 18650 cells cycled at elevated temperatures Part II. Capacity fade analysis.," *Journal of Power Sources,* vol. 112, pp. 614-620, 2002.

[149] I. Uchida, H. Ishikawa, M. Mohamedi, and M. Umeda, "AC-impedance measurements during thermal runaway process in several lithium/polymer batteries," *Journal of Power Sources,* vol. 119, pp. 821-825, 2003.

[150] H. A. Catherino, "Complexity in battery systems: thermal runaway in VRLA batteries," *Journal of Power Sources,* vol. 158, pp. 977-986, 2006.

[151] C. Y. Jhu, Y. W. Wang, C. Y. Wen, and C. M. Shu, "Thermal runaway potential of LiCoO2 and Li(Ni1/3Co1/3Mn1/3)O2 batteries determined with adiabatic calorimetry methodology," *Applied Energy,* vol. 100, pp. 127-131, 2012.

[152] K. W. Choi and N. P. Yao, "Heat Transfer in Lead-Acid Batteries Designed for Electric-Vehicle Propulsion Application," *Journal of Electrochemical Society,* vol. 126, pp. 1321-1328, 1979.

[153] R. J. Parise, "Quick Charge Battery With Internal Thermal Management," presented at the Energy Conversion Engineering Conference and Exhibit, 2000. (IECEC) 35th Intersociety Las Vegas, NV, 2000.

[154] T. M. Bandhauer and S. Garimella, "Passive, internal thermal management system for batteries using microscale liquid-vapor phase change," *Applied Thermal Engineering,* vol. 61, pp. 756-769, 2013.

[155] M. R. Cosley and M. P. Garcia, "Battery thermal management system," presented at the Proceedings of the INTELEC 26th annual international telecommunications energy conference, 2004.

[156] K. W. Choi and N. P. Yao, "Heat Transfer in Lead-Acid Batteries Designed for Electric-Vehicle Propulsion Application," *Journal of Electrochemical Society,* vol. 126, 1979.
[157] A. A. Pesaran, S. Burch, and M. Keyser, "An approach for designing thermal management systems for electric and hybrid vehicle battery packs," presented at the Fourth vehicle thermal management systems conference and exhibition, 1999.
[158] G. H. Kim and A. A. Pesaran, "Battery thermal management system design modeling," presented at the 22nd International Battery, Hybrid and Fuel Cell Electric Vehicle Conference and Exhibition, Yokohama, Japan, 2006.
[159] A. A. Pesaran, "Battery thermal management in EVs and HEVs: issues and solutions," presented at the Advanced Automotive Battery Conference, Las Vegas, Nevada, 2001.
[160] J. K. Kenneth and A. Rajagopalan, "Benchmarking of OEM hybrid electric vehicles at NREL," N. R. E. Laboratory, Ed., ed. Golden, Colorado, 2001.
[161] M. Zolot, A. A. Pesaran, and M. Mihalic, "Thermal evaluation of Toyata Prius Battery pack," presented at the Hyatt Crystal City: Future Car Congress, 2002.
[162] Brandbattery. (2012). *Photo Tour of Hybrid Batteries - Toyota Honda*. Available: http://www.brandbattery.com/photo-tour-of-hybrid-batteries/
[163] BEHR. (2009) Thermal Management for Hybrid Vehicles. *Technical Press Day*.
[164] K. J. Kelly, M. Mihalic, and M. Zolot, "Battery Usage and Thermal Performance of the Toyota Prius and Honda Insight during Chassis Dynamometer Testing," presented at the The Seventeenth Annual Battery Conference on Applications and Advances, Long Beach, California, 2002.
[165] P. Nelson, D. Dees, K. Amine, and G. Henriksen, "Modelling thermal management of lithium-ion PNGV batteries," *Journal of Power Sources,* vol. 110, pp. 349-356, 2002.
[166] Y. Lou, *Nickel-metal hydride battery cooling system research for hybrid electric vehicle*. Shanghai: Shanghai Jiao Tong University, 2007.
[167] A. Vlahinos and A. A. Pesaran, "Energy efficienct battery heating in cold climates," presented at the The future car congress, Arlington, Virginia, 2002.
[168] A. A. Pesaran, A. Vlahinos, and T. A. Stuart, "Cooling and preheating of batteries in hybrid electric vehicles," presented at the The 6th ASME-JSME Thermal Engineering Joint Conference, Hawaii Island, Hawaii, 2003.
[169] (2011). *Volvo C30 Electric equipped with three climate systems; bioethanol heater*. Available: http://www.greencarcongress.com/2011/03/c30-20110328.html
[170] M. Shimada, "A vehicle driven by electricity, designed for chill and snowy areas," *Sensors and Actuators A: Physical,* vol. 200, pp. 168-171, 2013.
[171] S. Kohn, G. Berdichevsky, and B. C. Hewett, "Tunable Frangible Battery Pack System," US Patent 7,923,144 B2, 2011.
[172] TESLA Roadster Analysis (in Chinese) [Online]. Available: http://wenku.baidu.com/view/c68f1d2b964bcf84b9d57bf3.html
[173] J. P. Rugh, A. A. Pesaran, and K. Smith, "Electric Vehicle Battery Thermal Issues and Thermal Management Techniques," presented at the SAE Alternative Refrigerant and System Efficiency Symposium, Scottsdale, Arizona USA, 2011.
[174] A. Jarrett and Y. Kim, "Design optimization of electric vehicle battery cooling plates for thermal performance," *Journal of Power Sources,* vol. 196, pp. 10359-10368, 2011.

[175] A. Faass and E. Clough, "Battery Module With Integrated Thermal Management System," US Patent 2013/0196184 A1, 2013.
[176] L. W. Jin, P. S. Lee, X. X. Kong, Y. Fan, and S. K. Chou, "Ultra-thin minichannel LCP for EV battery thermal management," *Applied Energy,* vol. 113, pp. 1786-1794, 2014.
[177] S. Al-Hallaj, "Safety and Thermal Management for Li-ion Batteries in Transportation Applications," presented at the EV Li-ion Battery Forum Europe 2012, Barcelona, Spain, 2012.
[178] S. Al-Hallaj and J. R. Selman, "A novel thermal management system for EV batteries using phase change material (PCM)," *Journal of the Electrochemical Society,* vol. 147, pp. 3231-3236, 2000.
[179] S. Al-Hallaj and J. R. Selman, "Novel thermal management of battery systems," 2002.
[180] S. A. Khateeb, M. M. Farid, J. R. Selman, and S. Al-Hallaj, "Design and simulation of a lithium-ion battery with a phase change material thermal management system for an electric scooter," *Journal of Power Sources,* vol. 128, pp. 292-307, 2004.
[181] R. Sabbah, R. Kizilel, J. R. Selman, and S. Al-Hallaj, "Active (air-cooled) VS passive (phase change material) thermal management of high power lithium-ion packs: limitation of temperature rise and uniformity of temperature distribution," *Journal of Power Sources,* vol. 182, pp. 630-638, 2008.
[182] Z. H. Rao, S. F. Wang, and G. Q. Zhang, "Simulation and experiment of thermal energy management with phase change material for ageing LiFePO4 power battery," *Energy Conversion and Management,* vol. 52, pp. 3408-3414, 2011.
[183] Z. G. Zhang and X. M. Fang, "Study on paraffin/expanded graphite composite phase change thermal energy storage material," *Energy Conversion and Management,* vol. 47, pp. 303-310, 2006.
[184] D. Zhang, S. L. Tian, and D. Y. Xiao, "Experimental study on the phase change behaviour of phase change material confined in pores," *Solar Energy,* vol. 81, pp. 653-660, 2007.
[185] X. Py, R. Olives, and S. Mauran, "Paraffin/porous-graphite-matrix composite as a high and constant power thermal storage material," *International Journal of Heat and Mass Transfer,* vol. 44, pp. 2727-2737, 2001.
[186] X. F. Zhou, H. Xiao, J. Feng, C. R. Zhang, and Y. G. Jiang, "Preparation and thermal properties of paraffin/porous silica ceramic composite," *Composites Science and Technology,* vol. 69, pp. 1246-1249, 2009.
[187] W. Q. Li, Z. G. Qu, Y. L. He, and W. Q. Tao, "Experimental and numerical studies on melting phase change heat transfer in open-cell metallic foams filled with paraffin," *Applied Thermal Engineering,* vol. 37, pp. 1-9, 2012.
[188] J. Fukai, M. Kanou, Y. Kodama, and O. Miyatake, "Thermal conductivity enhancement of energy storage media using carbon fibers," *Energy Conversion and Management,* vol. 41, pp. 1543-1556, 2000.
[189] E. B. S. Mettawee and G. M. R. Assassa, "Thermal conductivity enhancement in a latent heat storage system," *Solar Energy,* vol. 81, pp. 839-845, 2007.
[190] V. Shatikian, G. Ziskind, and R. Letan, "Numerical investigation of a PCM-based heat sink with internal fins," *International Journal of Heat and Mass Transfer,* vol. 48, pp. 3689-3706, 2005.

[191] A. Trp, "An experimental and numerical investigation of heat transfer during technical grade paraffin melting and solidification in a shell and tube latent heat thermal energy storage unit," *Solar Energy,* vol. 79, pp. 648-660, 2005.
[192] M. Akgun, O. Aydm, and K. Kaygusuz, "Thermal energy storage performance of paraffin in a novel tube-in-shell system," *Applied Thermal Engineering,* vol. 28, pp. 405-413, 2008.
[193] A. Alrashdan, A. T. Mayyas, and S. Al-Hallaj, "Thermo-mechanical behaviors of the expanded graphite-phase change material matrix used for thermal management of Li-ion battery packs," *Journal of Materials Processing Technology,* vol. 210, p. 6, 2010.
[194] G. H. Kim, J. Gonder, J. Lustbader, and A. Pesaran, "Thermal Management of Batteries in Advanced Vehicles Using Phase-Change Materials " *The World Electric Vehicle Journal,* vol. 2, pp. 134-147, 2008.
[195] W. Q. Li, Z. G. Qu, Y. L. He, and Y. B. Tao, "Experimental study of a passive thermal management system for high-powered lithium ion batteries using porous metal foam saturated with phase change materials," *Journal of Power Sources,* vol. 255, pp. 9-15, 2014.
[196] X. Duan and G. F. Naterer, "Heat transfer in phase change materials for thermal management of electric vehicle battery modules," *International Journal of Heat and Mass Transfer,* vol. 53, pp. 5176-5182, 2010.
[197] Z. H. Rao, *Research on heat transfer enhancement of lithium-ion power battery*. Guangzhou: Guangdong University of Technology, 2010.
[198] Z. H. Rao and G. Q. Zhang, "Thermal Properties of Paraffin Wax-based Composites Containing Graphite," *Energy Sources Part a-Recovery Utilization and Environmental Effects,* vol. 33, p. 7, 2011.
[199] X. Yang, Y.Y. Yan, D. Mullen, Recent developments of lightweight, high performance heat pipes, Applied Thermal Engineering, 33-34 (1) (2012), 1-14
[200] B. Jiang, Q. Wang and Y.Y. Yan, Efficient and integrated thermal management for electric vehicles, IMechE VTMS 12, 10-13 May 2015, Nottingham, UK
[201] Q. Wang, B. Jiang, Q.F. Xue, H.L. Sun, B. Li, H.M. Zou, Y.Y. Yan*, 2015. Experimental Investigation on EV Battery Cooling and Heating by Heat Pipes, Applied Thermal Engineering. 88 (5), 2015, 54-60.
[202] Y.Y. Yan, The challenge and opportunities – the integration of battery thermal management and air-conditioning for pure electric vehicles, keynote paper at VTI2012 Special Session of Thermal management, 16-19 July, 2012, Changchun.
[203] G. Swanepoel, *Thermal management of hybrid electrical vehicles using heat pipes*. University of Stellenbosch, 2001.
[204] M. S. Wu, K. H. Liu, Y. Y. Wang, and C. C. Wan, "Heat dissipation design for lithium-ion batteries," *Journal of Power Sources,* vol. 109, pp. 160-166, 2002.
[205] J. C. Jang and S. H. Rhi, "Battery thermal management system of future electric vehicles with loop thermosyphon," presented at the UK-Korea Conference on Science Technology and Entrepreneurship (UKC), 2010.
[206] V. Barantsevich and V. Shabalkin, "Heat pipes for thermal control of ISS solar battery drive," *Applied Thermal Engineering,* vol. 23, pp. 1119-1123, 2003.
[207] Y. J. Park, S. Jun, S. Kim, and D. H. Lee, "Design optimization of a loop heat pipe to cool a lithium-ion battery onboard a military aircraft," *Journal of Mechnical Science Technology,* vol. 24, pp. 609-618, 2010.

[208] G. Burban, A. Ayel, A. Alexandre, P. Lagonotte, Y. Bertin, and C. Romestant, "Experimental investigation of a pulsating heat pipe for hybrid vehicle applications," *Applied Thermal Engineering,* vol. 50, pp. 94-103, 2013.

[209] T. H. Tran, S. Harmand, B. Desmet, and S. Filangi, "Experimental investigation on the feasibility of heat pipe cooling for HEV/EV lithium-ion battery," *Applied Thermal Engineering,* vol. 63, pp. 551-558, 2014.

[210] Z. H. Rao, S. F. Wang, M. C. Wu, Z. R. Lin, and F. H. Li, "Experimental investigation on thermal management of electric vehicle battery with heat pipe," *Energy Conversion and Management,* vol. 65, pp. 92-97, 2013.